AD-A264 925

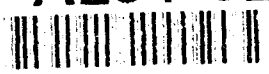

(1)

Dielectric breakdown and its influence on ignition

by

Dr M. M. Chaudhri (Principal Investigator)
Dr F. A. Al-Ramadhan
Mr I. U. Haq

Cavendish Laboratory
University of Cambridge
Madingley Road
Cambridge CB3 0HE

DTIC
ELECTE
MAY 2 6 1993
S A D

FINAL REPORT

Agreement No. D/ER1/9/4/2029/223/RARDE
1 April 1988 to 30th Sept 1992

March 1993

APPROVED FOR PUBLIC RELEASE
DISTRIBUTION IS UNLIMITED

93-11692

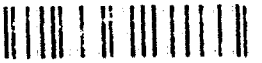

93 5 25 130

Dielectric breakdown and its influence on ignition

b y

Dr M. M. Chaudhri (Principal Investigator)
Dr F. A. Al-Ramadhan
Mr I. U. Haq

Cavendish Laboratory
University of Cambridge
Madingley Road
Cambridge CB3 0HE

FINAL REPORT

Agreement No. D/ER1/9/4/2029/223/RARE
1 April 1988 to 30th Sept 1992

March 1993

Accession For
NTIS
DTIC
Unannounced
Justification
By
Distribution/
Availability Codes
Dist | Avail and/or Special
A-1

List of contents

	Page
Abstract	1
Dielectric breakdown and its influence on ignition	
Introduction	2
Experimental	3
Results	6
Discussion	10
Conclusions	12
References	13
Figure captions	14
Low energy laser ignition of magnesium-teflon-viton compositions	
Introduction	18
experimental	20
Results	23
Discussion	26
Conclusions	28
References	29
Acknowledgements	30
Figure captions	-

Abstract

Electrical conduction, dielectric breakdown and the consequent ignition of small pellets, 0.2 to 5 mm in thickness and 5 to 7 mm in diameter, of MTV compositions SR886B, SR886E and SR886E have been investigated. The investigations were made using d.c fields and high-speed photography at framing rates of up to one million frames per second was employed to follow the breakdown and ignition behaviour. It was found that under suitable conditions, the dielectric breakdown of the samples led to their ignition and the delay time between the breakdown and ignition could be as small as 20 - 25 μs. Furthermore, a special circuit was designed and constructed for determining the minimum ignition energies of samples of different thicknesses. It was found that for samples of thickness of ~ 0.2 mm the minimum electrostatic energy which could cause ignition was as low as ~ 1 mJ. Moreover, the minimum ignition energy was found to increase with the sample thickness. A model, based on our previous model for the electrical ignition of silver azide, has been proposed. According to this, the dielectric breakdown leads to the formation of high conductivity filaments in which Joule heating results in the formation of high temperature hot spots. Ignition initiates at these hot spots. An essential feature of this model is that the dielectric breakdown is a prerequisite for electrical ignition.

Ignition of unconfined pellets of magnesium-teflon-viton compositions by unfocused low energy non-Q-switched Nd /Glass laser pulses of wavelength 1060 nm has also been investigated using high-speed framing photography. Ignition has been found to initiate at localised sites which are probably centred on the magnesium particles in the compositions. Ignition was obtained for an estimated absorbed energy of 7.6 ± 0.6 mJ when a 3 mm diameter area of the test sample was irradiated with the laser beam and the time delay between the start of the laser pulse and the initiation of ignition was 20 μs. By comparing the delay time to ignition with that predicted by the adiabatic explosion theory, it is concluded that the mechanism of ignition by laser irradiation is thermal in origin.

Dielectric breakdown and its influence on ignition

M M Chaudhri, F A Al-Ramadhan and I U Haq
Cavendish Laboratory, Madingley Road, Cambridge

1 Introduction

Magnesium-teflon-viton (MTV) compositions consist of viton-coated magnesium and teflon particles. These compositions are capable of sustaining fast reactions, giving rise to high temperatures and thus are of considerable practical importance. They are often used in a pellet form, which is produced by compacting the loose composition in specially constructed metallic dies. During the last few years a number of unexplained ignitions of the compositions, during the compaction and pellet-ejection stages, has been reported.[1,2] The cause of the ignitions has not been understood fully so far. Some investigators have speculated that electrostatic charging during the compaction stage may be responsible for the ignitions.[3] However, some previous work suggested that the ignition of these compositions by electrostatic discharges of energies less than 1.5 J could not be caused.[4] It has also been proposed that pyrophoric and piezoelectric effects may be responsible[5], but experimental observations supporting this proposal have been lacking.

In order to investigate any correlation between the electrostatic charging of MTV pellets during compaction and their ignition, we have carried out a research programme in which detailed studies of the electrical conduction, dielectric breakdown behaviour, minimum ignition energies, and high-speed photography of the ignition processes have been carried out. Some preliminary results from these studies were presented at a recent conference.[6] Our experiments have shown that electrostatic energies as small as ~ 1 mJ can cause ignition of a thin pellet of the MTV compositions and that the time delay between the dielectric breakdown and ignition can be as small as a few microseconds.

In a parallel series of experiments, pellets of the compositions have also been ignited with non-Q-switched pulses from a Nd/glass laser. In these experiments as well we measured the minimum energies absorbed by a sample, which could give rise to ignition. Moreover, high-speed photographic work showed that the delay time between the irradiation and ignition was a

few microseconds, similar to the time delay determined in the electrical work. Both the electrical ignition and the laser ignition investigations are described below separately.

2 Experimental

The magnesium-teflon-viton compositions of types SR886B, SR886F, and SR886E used in this work were supplied in the form of loose powders and cylindrical pellets. The weight per cent ratios of Mg, teflon, and viton in the compositions were roughly 55:45:5, respectively. The Mg particle sizes were in the range of less than 1 μm to several tens μm. The pellets were 5mm in diameter and 1 to 5mm in thickness and all of them had been compacted to a pressure of 4 tons.in^{-2} using a punch speed of 3 mms^{-1} Before compaction, the Mg and PTFE particles were coated with viton (the viton used was not pure and had unknown impurities). The coating of the Mg particles with the viton had a beneficial effect in that the water of the atmosphere did not react with the Mg surface. Scanning electron micrographs of uncoated Mg particles of different grades are shown in Fig.1(a, b) and Fig.2(a, b). We note that whereas the particles of the mixed grade and grade 6 are spherical, those of the cut grade have sharp points and edges. Fig.3(a, b) shows uncoated PTFE particles used in the compositions. Using a transmission electron microscope, we were able to make an estimate of the viton coating on the Mg particles. A bright field mode electron micrograph of a typical Mg particle coated with viton is shown in Fig.4(a); here the entire particle (i.e., Mg plus viton) looks dark. When an electron micrograph was taken in the dark mode, the viton coating gave a much lighter image (see at (b) in Fig.4(b)). From these types of electron micrograph, we determined the thickness of the viton coating on the Mg particles to be in the range of 0.5-1.0 μm. SEM micrographs were also taken of pellets of compositions of the various types. Typical micrographs are shown in Figures 5, 6, and 7 from which we estimate that on average the Mg particles are separated from one another by a 2-3 μm thick layer of the PTFE and viton.

Some pellets, 7mm in diameter and thickness in the range of 0.075 to 2.7mm were made in the laboratory using a compaction pressure of 4 tons.in^{-2}. RARDE also supplied some 5mm diameter MTV pellets containing up to 10% by weight of copper particles.

To measure the electrical characteristics of the pellets, a schematic diagram of the circuit used is shown in Fig.8. On each flat side of the test pellet, a

platinum disc 5mm in diameter and 0.125mm in thickness was placed and the sandwich was planed between a flat brass plate and 3mm diameter brass hemisphere, which was ground on one end of a brass rod 5mm in diameter and 50mm in length, the latter could be gently pressed onto the test sample to make good-quality electrical contacts. A d-c power supply (Fluke 415B), capable of delivering continuously variable voltage in the range of 0-3.1 kV at a maximum current of 30 mA, was employed. The sample current was monitored with a Keithley digital electrometer (model 616B). In some cases, another electrometer (Keithley, model 480) was used. The output of the electrometer was recorded on a chart recorder. The circuit also contained a wire-wound current-limiting series resistance of 150 kΩ. Its main purpose was to protect the sensitive electrometers in case of a dielectric breakdown of the test sample. In order to examine any rapid changes in the current through the test sample, the voltage drop across a smaller (i.e., 10 kΩ) resistance was monitored on a storage oscilloscope (Gould, model 4035). In some cases, when the value of the applied voltage was well below the breakdown value, the current-limiting resistance was reduced to 5.1 kΩ and the electrometer was taken out of the circuit and instead the sample current was monitored by measuring the voltage drop across the 10 kΩ resistance.

Using this circuit and the 150 kΩ series resistance, any dielectric breakdown of the test sample was unable to lead to its ignition. Without the 150 kΩ series resistance, the dielectric breakdown of the test sample often resulted in its ignition.

The ignition behaviour of the MTV pellets due to their dielectric breakdown was studied with the circuit shown in Fig.9. Again, the electrodes and the electrical contacts of the test sample were the same as those shown in Fig.8. However, the voltage to the test sample was applied very rapidly (i.e., within ~ 2μs) from a charged capacitor, C, by employing a thyratron switch in the circuit. By using capacitors of different capacitances in the range of 1175 to 10,670 PF, the response of the test sample to different energies passing through it could also be studied. To charge the capacitor to a predetermined voltage, the manual switch, S, was closed and the thyratron switch kept in the 'off' position. After the capacitor, C, was fully charged, the switch, S, was cut out and the thyratron switch switched on using either a -5V trigger pulse or manually triggering it. The switching on of the thyratron valve immediately (i.e., within ~ 2μs) caused the application of the capacitor voltage across the test

sample. The thyratron trigger pulse also triggered a dual beam storage oscilloscope (Gould model 4035), which continuously recorded the voltage across the sample as well as the current through it (i.e., the voltage drop across R_2, a 1 Ω resistance). By using capacitors of different values and by charging them to different voltages, the critical energy values, which caused samples' ignition were thus determined.

The ignition of a sample produced visible light and in some cases the time delay between the application of the voltage across the test sample and its ignition was recorded with a fast response photo diode (BPX 65) placed close to the sample.

High-speed framing photography up to framing rates of 1 million frames per second was also employed to study the dielectric breakdown and ignition processes of the MTV pellets. A schematic diagram of the experimental arrangement used is shown in Fig.10. Basically, the electrical circuit was the same as that shown in Fig.9, but for the high-speed photographic purpose the thyratron switch was triggered electrically by an output pulse from a 3-channel delay unit (John Hadland type JH-TDG.XLD10), which itself was triggered manually. Another output pulse from the delay unit triggered an external light source (Bowens Mono 400D) and the third pulse triggered an Imacon (790) image convertor framing camera. In this way the application of the voltage across the sample, the light-flash from the flash unit, and the Imacon camera were synchronized. A few experiments were carried out in which the Imacon camera was replaced by a high-speed video camera (Ekta-Pro, Kodak) working at a framing rate of 500 frames per second.

From the fact that in the MTV compositions the viton surrounded the Mg and PTFE particles, any dielectric breakdown of the compositions must also involve the dielectric breakdown of the viton. Therefore a few experiments were conducted in which the breakdown of transparent samples of viton of dimensions 3mm x 2mm x 2mm and containing Mg particles was examined *in situ* under an optical microscope using transmitted light. The Mg particles were introduced into the viton samples by placing them onto a large face (3mm x 2mm) of the sample and then covering them with a small drop of acetone. As the acetone dissolved the viton, the Mg particle subsided to about 20-30 μm below the sample surface. The acetone was then allowed to evaporate away. Electrical connections were made on the 2mm x 2mm faces using silver dag

and a d.c. field of 3 MVm^{-1} was applied and visual observations of any changes in the sample were continually made over several hours.

3 Results

For low applied d.c. fields (i.e. 100 kVm^{-1}) across pellets of the various types of MTV composition, the current increased linearly with increasing voltage. An example is shown in Fig.11; here the sample was made of the MTV (type E) composition and its dimensions were 5mm in diameter and 2mm in thickness and the circuit (shown in Fig.8) contained the 150 kΩ current-limiting series resistance. At higher fields the current increased non-linearly with the applied voltage and at still higher fields, the sample current exhibited rapid fluctuations. However, at this stage the mean level of the current, at a given applied field, did not increase with increasing time. An example is shown in Fig.12. As the applied field was increased still further, the current fluctuations at a constant applied field became more frequent and the sample current increased with increasing time; if the current-timing limiting resistance were not in series, or the value of the resistance was smaller (5.1 kΩ), the sample would eventually break down, possibly leading to an ignition. An example is shown in Fig.13. Here the sample was 5mm diameter of 4mm in thickness, the applied voltage was 2.3 kV, and the value of the current limiting resistance was 5.1 kΩ. The figure clearly shows violent current fluctuations, leading to ignition about 1500 μs after the application of the field. Before the occurrence of the dielectric breakdown and for d.c. fields of up to ~ 100 kVm^{-1} the sample conductivity was $1.2 \times 10^{-10}\ \Omega^{-1}m^{-1}$. After the breakdown, the electrical resistance does not become zero. In fact, for low applied fields, the current in a broken-down sample increases linearly with increasing voltage and the effective conductivity becomes $3.25 \times 10^{-3}\Omega^{-1}m^{-1}$, which is an increase of 7 orders of magnitude over that of a fresh sample.

Electrically broken-down samples often showed a memory effect; if after the initial breakdown of a sample the field was removed for a period of 20s or more and the same field re-applied, the initial current at the time of the reapplication of the field was several orders of magnitude smaller than the value reached during the breakdown. However, when the field remained applied for a few seconds, the current increased rapidly towards the value reached during the first breakdown. An example of such behaviour is shown in Fig.14. Here the sample was of the MTV (type F) composition having a diameter of 5mm and thickness of 2mm; in the presence of the 150 kΩ series

resistance, it had been broken down by the application of a d.c. voltage of 3 kV. The field was then removed from the sample. After a period of ~ 1 minute, a d.c. voltage of 1100 volts was applied and the sample current was monitored by measuring the potential drop across the 10 kΩ series resistance using the storage scope. It will be seen from Fig.14 that initially, the current is ~ 2.5×10^{-8}A, but after ~ 9 s, the current jumps to ~ 1 mA. It is because of this type of memory effect that it was not possible to measure reliably the resistance of a broken down sample using ordinary resistance meters.

The MTV samples containing small proportions of copper particles showed I-V characteristics for low applied fields quite similar to those of the MTV compositions without the copper particles. Typical behaviour of a 5mm diameter and 1mm thick pellet of the MTV composition SR886E mixed with 1% by weight of the copper particles is shown in Fig.15. The behaviour below ~ 100 kVm^{-1} is reasonably linear, and the sample has a conductivity of 1.4×10^{-10} $\Omega^{-1}m^{-1}$; this value is only slightly higher than the conductivity of the MTV samples without any copper particles, However, in the case of the MTV pellets containing 7% and 10% copper particles, the pre-breakdown conductivities were markedly higher with value of 1.86×10^{-7} and $6.65 \times 10^{-1}\Omega^{-1}m^{-1}$, respectively. Another consequence of the addition of the copper particles was the reduction in the values of the breakdown fields, which were typically 0.8, 0.1 and 0.035 MVm^{-1} for the MTV samples containing 1%, 7%, and 10%, copper respectively. The conductivities of the broken down MTV samples containing the copper particles were, however, about 20 times higher than that of the broken down MTV pellets without any copper particles (see Table 1).

When the samples were examined using the circuit shown in Fig.9, it was found that the breakdown occurred within microseconds of the application of the field. Typical breakdown behaviour of an MTV (type F) pellet, 5mm in diameter and 1mm in thickness, is shown in Fig.16; the breakdown occurs after ~ 23 μs the application of the field, resulting in rapid current fluctuations, marked rise in the sample current, and accompanying voltage drop across the sample. In this case the sample also ignited. In fact, generally, the ignition occurred within microseconds of the electrical breakdown, as confirmed using a photo detector and high-speed photography. Fig. 17 gives an example showing the time delay between the moments of the dielectric breakdown and the detection of the light (i.e., due to the ignition) from the sample. The entire

sample was consumed and that is why the photo diode signal remains high well after the sample current has decayed to zero after the breakdown.

A high-speed photographic sequence taken at 1 x 10^6 frames per second of the breakdown and consequent ignition of a 2mm thick pellet of MTV (type SR886F) composition due to the discharge of 0.05 μF capacitor charged to 3.1 kV through it is shown in Fig.18. Frame 1 was taken 23.5 μs after the application of the field, and in frame 5 light is emitted from localised hot spots (see at arrows), at the contacts between the electrodes, and the specimen. In the subsequent frames (i.e., frames 6-8) two of the 'hot spots' extinguish, whereas the third one continues to grow and the entire sample was consumed. The emitted light is thought to be an indication of ignition of the sample. The current-time and voltage-time characteristics of the sample are shown in Fig.19(a) and (b). It will be seen that the dielectric breakdown, as indicated by the sudden rise of the current and the drop in the voltage, occurs after a delay of 26-27 μs; this time delay value is in agreement with that estimated from the high-speed photographic sequence. Fig. 19(b) shows higher time resolution behaviour in the sample current and the voltage across it; note that at the breakdown, the rapid current fluctuations occur with a frequency of 2-3 Mcs^{-1}.

Another sequence taken at 1 million frames per second of the dielectric breakdown and ignition of a 3mm thick and 5mm diameter pellet of the MTV (type F) composition by the discharge of a 0.05 μF capacitor charged to 2kV through it is shown in Fig.20. The field was applied 22 μs before frames 1 and it will be seen from this frame that quite intense light emission occurs at the contact regions at the left hand side of the sample. In frame 2, the intensity of the light has diminished considerably and a crack has appeared in the sample, which leads to a small fragment of the sample being ejected from the sample at a speed of ~ 170 m s^{-1} (see at arrow in frame 8). It appears from frames 3-8 that the reaction may have ceased to propagate. In fact, it was not extinguished and the entire sample was consumed.

It may be thought that the breakdown experiments conducted in air, which result in the ignition of the sample, might be helped by the ambient oxygen in causing ignition. Therefore, a few experiments were conducted in which the test sample was immersed in transformer oil to eliminate any effects of the ambient oxygen. It was found that the breakdown and ignition characteristics of the MTV samples were similar in air and in the transformer oil. A typical

sequence of high-speed photographs taken at 50.000 frames per second of the dielectric breakdown and ignition of an MTV (type F) sample under oil is shown in Fig.21. The interframe time is 20 μs. The field was applied to the sample by discharging a 0.05 μF capacitor charged to 3 kV 20 μs before frame 1. In frame 2, clouds of the reaction products can be seen at the contact regions between the sample and the electrodes. We estimate a time delay of ~ 40 μs between the application of the field and the initiation of ignition. In the rest of the frames (i.e., frames 3-8), the reaction continues to grow in the sample. In this sequence, the emission of light at the instant of the breakdown is considerably less than when the experiment is conducted in air. However, it was confirmed from high-speed video sequences taken at 500 frames per second that at the contact regions between the sample and the electrodes light is indeed emitted, even when the sample is immersed in transformer oil, at the moment of breakdown and ignition. A selected frame from a sequence is shown in Fig.22. Here the sample was a 2mm thick and 5mm diameter pellet of the MTV (type E) composition and it was broken down by discharging a 0.05 μF capacitor charged to 3 kV through it, the emitted light is shown by arrow. It may be added that the samples' current-time and voltage-time curves for this experiment were very similar to those shown in Fig. 19(b). Experiments were also conducted in which the ambient gas was argon and it was found that in these experiments as well the breakdown and ignition were accompanied by the emission of light.

It was said in the above that occasionally the breakdown caused fragmentation of the sample; this process sometimes led to the cessation of the reaction and the undecomposed parts of the sample were recovered. An example is shown in Fig.23.

The minimum ignition energies of pellets of different sizes and of different compositions were determined using the experimental arrangement shown in Fig.9. The results are shown in Table 2, from which it will be seen that the thicker the sample, the greater is the required minimum energy for ignition. In the case of the pellets of the MTV (type F) composition, the variation of the minimum ignition energy with pellet thickness is also shown in Fig.24. It is interesting to note that electrical energy as small as 1.18 mJ can cause ignition. The breakdown field was also found to depend upon the pellet thickness; the results are given in Table 3 and it will be seen that as the thickness increases,

the average critical breakdown field generally decreases a little for all three types of composition.

The breakdown behaviour of small transparent samples of the viton containing a few Mg particles, ~ 12 μm in diameter, was interesting. For a sufficiently high field, the viton around the Mg particles degraded (possibly due to decomposition) as indicated by the formation and growth of 'tree-like' structures. An x-ray microprobe examination indicated that these 'tree-like' structures did not contain any Mg. In the presence of the critical field these structures would link together different Mg particles and thus may eventually provide very low resistance paths between the electrodes. We call these structures 'conducting' filaments and believe that they play a vital role in the processes of the breakdown and ignition. A typical photomicrograph of a 'tree-like' structure around an Mg particle embedded in the viton is shown in Fig.25(a); here an average electrical field of 3 MVm^{-1} had been applied to the sample for ~ 10 hours, and the resulting treeing is shown at arrows. The treeing from the particle grew towards the anode. A photomicrograph of the treeing at another Mg particle is shown in Fig. 25(b). Here a bubble (see at (b)) also formed. A Mg particle is shown at (a) and the tree is labelled as C. Occasionally sparking was observed within the bubble. This produced bluish-white light.

4 Discussion

The experiments described in the above have shown that the dielectric breakdown of small unconfined samples of the MTV compositions (SR886, types B, E and F) can lead to their ignition. Without the electrical breakdown of the samples, it has not been possible to ignite them by an electric field. Moreover, the breakdown field values of 0.1 - 2 MV m^{-1} are quite low compared with those for the alkali halides (100 MV m^{-1}) or pure polymers (500-1500 MV m^{-1}). These rather low breakdown field values may be a consequence of the nature of the MTV compositions in which about 10 μm diameter magnesium spheres are separated from one another by about 3 μm thick layers of viton and PTFE. It appears quite likely that the breakdown process of the insulating polymer layer begins at the surface of the magnesium particles resulting in the formation and development of the 'treeing'.[7] The initiation of such 'treeing' at the Mg particles is shown in Figs. 25 (a,b). The metallic particles locally enhance the field and when this enhanced field becomes large enough, the process of 'treeing' begins. It also appears that the 'treeing' is

formed by the decomposition of the polymeric material, a main product of which is a carbonaceous material, which is electrically conducting. Thus 'treeing' gives rise to conducting filaments. With increasing time in the presence of the critical field, the conducting paths grow in size. Once a continuous path of such filaments forms between the two electrodes, Joule heating will give rise to 'hot spots' along the filaments. If the temperatures of the hot spots are sufficiently high, ignition of the sample will occur. It appears that in these compositions fast reactions can grow throughout a sample from hot spot regions as small as a few μm. The 'filament' mechanism here is based on our proposed mechanism for the dielectric breakdown and explosion of silver azide.[8,9]

The electrical conductivity of the fresh sample of MTV is ~ 10^{-10} (Ωm^{-1}); when particles of copper were added to these, the conductivity increased to ~ 10^{-7} (Ωm^{-1}) (see Table 1). It may be thought that this higher conductivity material may be more effective in dissipating any electrostatic charges and thus it would be relatively safe. However, this may not be so as MTV compositions containing copper particles breakdown and ignite at considerably lower electrical fields. In the case of the pellets of MTV compositions, electrostatic surface potentials of 3600 V have been reported.[1] At present such measurements of MTV compositions containing copper particles have not been made.

Evidence in support of the existence of the highly conducting filaments in a broken down sample comes from the conductivity experiments conducted at different temperatures.[6] The broken down samples were shown to possess metallic conduction behaviour.

Now we make a few comments on the recovery of the sample resistance after its initial breakdown (see Figs. 12 and 14). It is possible that during the process of the treeing, the surrounding polymer material becomes mechanically stressed and when it relaxes, a physical disruption of any high-conductivity filaments may take place. This will result in the recovery of the resistance.

Our minimum ignition energy measurements have proved very successful. We found that the value of the minimum ignition energy increases from ~ 1mJ for a 240 μm thick pellet of 7mm in diameter to 34 mJ for a pellet of 4mm in thickness (see Table 2 and Fig.24). This increase of the minimum energy

with increasing sample thickness can be explained on the fact that a thicker sample will necessarily have a longer filament joining the two electrodes. If the diameter of a critical filament and the current through it are the same and are independent of the MTV sample thickness, then the total energy dissipation necessary for ignition will increase with sample thickness.

Our high-speed photographic sequences have shown that the ignition of the MTV samples takes place within ~ 20 μs of its dielectric breakdown. These observations fit in with our conducting filament model in which high temperatures are created at the instant of the dielectric breakdown. These temperatures must be several thousand degrees in order to give rise to such short time delays. Our laser ignition experiments, described in Section 2, further support the hypothesis of high temperatures during the breakdown.

Finally, the model presented in the above can be applicable to explosive compacts containing metallic particles. In order to avoid electrostatic ignitions, one method would be to use much higher dielectric strength coatings on the Mg particles. Another possibility is to use sufficient amounts of conducting polymers in the pellets so that no electrostatic charge can accumulate on them. However, future experiments will show the most appropriate conditions for avoiding accidental ignitions.

Conclusions

1. Dielectric breakdown of MTV compositions does cause their ignition.

2. The minimum ignition energies depend upon sample thickness and can be as low as ~ 1 mJ.

3. Delay times to ignition can be as low as a few microseconds.

4. Increasing the conductivity of a sample by the addition of extra metallic particles can lead to an increased electrical sensitivity.

5. We envisage that composites of propellants/secondary explosives/metal particles may behave similarly to the MTV compositions.

References

1. Dierks, B V, *Journal of Hazardous Materials*, **13**, 3-15, (1986).

2. Dierks, B V, Electrostatic Sensitivity of Consolidated Magnesium-Teflon Compositions, Morton Thiokel Inc. Report, Longhorn Division, Marshal, Texas (as quoted in reference 5).

3. Bibby, M J, RARDE Divisional Working paper, 1/84 (XM3) (1984).

4. Hearn, G, Wolfson Electrostatics Advisory Unit. Report Nos G86/A336, G86/D401, G86/K428 and G88/476B.

5. Hearn, G L, Sing, S; Hazards from Electrostatics in the Manufacture of Infra-red Decoy Flares. Inst. Phys. Conf. Ser. No.85: Section 3. "Electrostatics '87", Oxford, IOP Publishing Ltd., 1987, pp 2290234.

6. Haq, I U, and Chaudhri, MM, 14th International Pyrotechnics Seminar, Jersey, 18-22 September 1989, pp 135.

7. Seanor, D A; Electrical Properties of Polymers, Academic Press, INC. (London) Ltd. (1982) pp 341-346.

8. Tang, T B, and Chaudhri, M M, *Nature*, **282**, 54, (1979).

9. Tang, T B, Chaudhri, M M, *Phys.Rev. B*, **30 (10)**, 6154-6164 (1984).

Figure Captions

Figure 1
Scanning electron micrographs of the uncoated Mg particles. (a) - Mixed grade; (b) - grade 6.

Figure 2
Scanning electron micrographs taken at two different magnifications of the uncoated Mg particles of the cut grade. Sharp edges and fine corners can be easily seen in the higher magnification micrograph.

Figure 3
Scanning electron micrographs taken at two different magnifications of the PTFE particles.

Figure 4
Transmission electron micrographs of a viton-coated Mg particle taken in (a) the bright mode and (b) in the dark mode. In the latter the viton layer, 0.5-1.0 μm thick, is indicated by an arrow at (b).

Figure 5
Scanning electron micrograph of a sectioned surface of a pellet of SR886B. The arrows indicate polymer strands, which may have formed during the compaction or sectioning stages.

Figure 6
Scanning electron micrograph of a sectioned surface of an MTV pellet of composition SR886F.

Figure 7
Scanning electron micrograph of a flat surface of a compacted pellet of an MTV SR886E composition.

Figure 8
Schematic diagram of the electrical circuit used for investigating the d.c electrical conductivity and dielectric breakdown of MTV pellets.

Figure 9

Schematic diagram of the electrical circuit used for measuring the minimum electrical energies required for igniting pellets of the MTV compositions.

Figure 10

Schematic diagram of the experimental arrangement used for the high-speed photography of the dielectric breakdown and consequent ignition of the MTV compositions.

Figure 11

D.C current-voltage characteristics of a fresh pellet (i.e., before breakdown) of the MTV composition SR886E. Pellet diameter: 5mm; thickness: 2mm.

Figure 12

Current vs time behaviour (using the circuit shown in Fig.8) of a fresh 1mm thick and 5mm diameter pellet of the MTV composition SR886E when a d.c. voltage of 580 V was applied across its thickness.

Figure 13

Current vs time behaviour (using the circuit shown in Fig.8, but having a series resistance of only 5.1 kΩ) of a fresh 4mm thick and 5mm diameter pellet of the MTV composition SR886E when the d.c. applied voltage was 2.3 kV.

Figure 14

Memory effect. Using the circuit shown in Fig.8, a 2mm thick and 5mm diameter pellet of the MTV composition SR886F was broken down by a d.c. voltage of 3 KV applied across the flat faces. Because of the current-limiting series resistance of 150 kΩ the sample did not ignite. The field was removed and a small d.c. voltage of 1.1 kV applied after a period of ~ 20s. For the first 8 seconds, the current through the sample remained low as if the sample resistance had recovered. However, within the next two seconds the current suddenly jumped to 1 mA.

Figure 15

D.C current-voltage characteristics of a 1mm thick and 5mm diameter pellet of the MTV composition SR886E containing 1% by weight copper particles.

Figure 16

Current-voltage characteristics of the dielectric breakdown and ignition of a 2mm thick and 5mm diameter pellet of the MTV composition SR886F due to the discharge of a 0.05 μF capacitor charged to 3 kV through it. Here the circuit shown in Fig.9 was used.

Figure 17

Dielectric breakdown and ignition of a 3mm thick and 5mm diameter pellet of the MTV composition SR886F as detected with a fast response time photo diode. The circuit shown in Fig.9 was used; the discharge capacitor was 0.05 μF and it was charged to 3 kV. The photo diode signal starts increasing soon after the sample current reaches the maximum value.

Figure 18

High-speed photographic sequence of the dielectric breakdown and ignition in air of a 2mm thick and 5mm diameter pellet of the MTV composition SR886F. The circuit shown in Fig.9 was used; the discharge capacitor was 0.05μF and it was charged t 3.1 kV. The field was applied 23.5 μs before frame 1 and the ignition is initiated in frame 5 (see at arrows). Interframe time: 1 μs.

Figure 19

Current-voltage characteristics of the dielectric breakdown of a 2mm thick and 5mm diameter pellet of the MTV composition SR886F due to the discharge of a 0.05 μF capacitor charged to 3.1 kV through it. The inset shows a higher time resolution of the sample current, which has a 2 Mcs^{-1} frequency.

Figure 20

High-speed photographic sequence of the dielectric breakdown and ignition in air of a 3mm thick and 5mm diameter pellet of the MTV composition SR886F. The circuit sown in Fig.9 was used; the discharge capacitor was 0.05 μF and it was charged to 2 kV. The field was applied 20 μs before frame 1, and the dielectric breakdown leads to fracturing of the sample (see at arrow in frame 5). Interframe time: 1 μs.

Figure 21

High-speed photographic sequence of the dielectric breakdown and ignition under transformer oil of a 2mm thick and 5mm diameter pellet of the MTV composition SR886F. The circuit shown in Fig.9 was used; the discharge capacitor was 0.05 μF and it was charged to 3 kV. The field was applied 20 μs before frame 1 and the ignition begins in frame 2 (see at arrows). Interframe time: 20 μs.

Figure 22

A selected frame from a high-speed video sequence of the dielectric breakdown and ignition under transformer oil of a 2mm thick and 5mm diameter pellet of the MTV composition SR886E. The circuit shown in Fig.9 was used; the discharge capacitor was 0.05 μF and it was charged to 3 kV. Emission of light due to the breakdown and ignition is shown at arrow. Framing rate: 500 frames per second.

Figure 23

A crater formed due to a microexplosion, caused by the dielectric breakdown, in an MTV pellet (SR886E), 1mm in thickness and 5mm in diameter. A piece of the composition, thrown out of the sample due to the microexplosion, is shown in (a), whereas the original sample with the crater is shown in (b).

Figure 24

The variation of the minimum ignition energy (electrostatic) with the thickness of pellets of the MTV composition SR886F. The pellet diameter was 7mm and the circuit shown in Fig.9 was used.

Figure 25

Formation of conducting 'treeing' in a thin layer of viton containing Mg particles when it had been subjected to a d.c field of 3 MV m^{-1} for several hours. In (a) the 'trees' are the dark features shown at arrows; these grew in size towards the anode. In (b) is another 'tree' (see at (c)) along with a bubble (see at (b)) that was formed during the electrical degradation process; an Mg particle is shown at (a).

Table 1. Conductivity values before and after dielectric breakdown in different MTV and PTFE samples from different batches. These values were calculated from the linear part of the current / voltage characteristics which was obtained using the d.c. circuit shown in figure 8.

batch No.	Pellet type	Pellet thickness / mm	breakdown voltage /kV ± 0.25%	breakdown field / MVm^{-1} ± 1%	No. of samples tested	Conductivity before breakdown / $\Omega^{-1} m^{-1}$	Conductivity after breakdown / $\Omega^{-1} m^{-1}$ ± 5.5%
FA/47/91	SR886E	1	3	3	10	1.18×10^{-10} ± 5.5%	3.25×10^{-3}
FA/159/89	SR886E+ Cu, mix 3 (99%MTV+ 1%Cu)	1	0.8	0.8	6	1.44×10^{-10} ± 5.5%	1.41×10^{-2}
FA/219/89	MTV+Cu mix 2 (93%MTV+ 7%Cu)	2	0.2	0.1	8	1.86×10^{-7} ± 2.3%	1.38×10^{-2}
FA/01/90	MTV+Cu (92.5%MTV +7.5% Cu)	2	0.07	0.035	7	6.65×10^{-7} ± 2.3%	1.1×10^{-2}
FA/47/91	SR886F	2	1.2	0.6	10	1.63×10^{-10} ± 5.5%	1.24×10^{-2}
	PTFE coated viton	1	2.5	2.5	8	1.37×10^{-10} ± 5.5%	8.04×10^{-4}
	PTFE tape	75 µm	1.2	16	6	7×10^{-12} ± 5.5%	2.37×10^{-4}

Table 2. Minimum ignition energy values for MTV compositions, using the thyratron switch.

MTV type- thickness /diameter / mm	Applied voltage / V	Capacitor used / nF ± 5%	min.energy 1/2 C V^2 / mJ ± 5%	Event
F– 0.24 / 7	600	6.6	1.18	ignition
F– 0.3 / 7	800	=	2.1	=
F– 0.45 / 7	900	=	2.67	=
F– 0.7 / 7	1000	=	3.3	=
F– 0.75 / 7	1100	=	4.0	=
F–1 / 5	830	17	5.87	=
F–2 / 5	900	=	6.88	=
F–2.7 / 7	1500	6.6	7.4	=
F–3 / 5	1400	=	16.6	=
F–4 / 5	2000	=	34	=
B–1 / 5	1500	20	22.5	=
B–2 / 5	2800	17	66.6	=
B–3 / 5	3000	=	76.5	=
E-0.45 / 7	1500	6.6	7.4	=
E–1 / 5	2550	20	65	=
E–2,3,4 / 5	3000	17	—	no ignition

Table 3. Breakdown voltages and fields values for MTV samples of different types as a function of pellet thickness. These data were obtained using d.c. voltage application.

MTV type– thickness / mm	Breakdown voltage / V ± 0.25% 1st , 2nd sample	Breakdown field / MV m^{-1} ± 0.25% 1st , 2nd sample	Average breakdown field / MV m^{-1} & Event
F– 1	700, 700	0.7, 0.7	
F– 2	1400, 1500	0.7, 0.75	0.678 ± 0.02
F– 3	2100, 2100	0.7, 0.7	
F– 4	2700, 2000	0.675, 0.5	
B– 1	1300, 1800	1.3, 1.8	1.5 ± 0.1
B– 2	3000, 2800	1.5, 1.4	
B– 3&4	3100, 3100		no breakdown
E– 1	2200, 1900	2.2, 1.9	1.7 ± 0.25
E– 2	2700, 2700	1.35, 1.35	
E– 3&4	3100, 3100		no breakdown

(a)

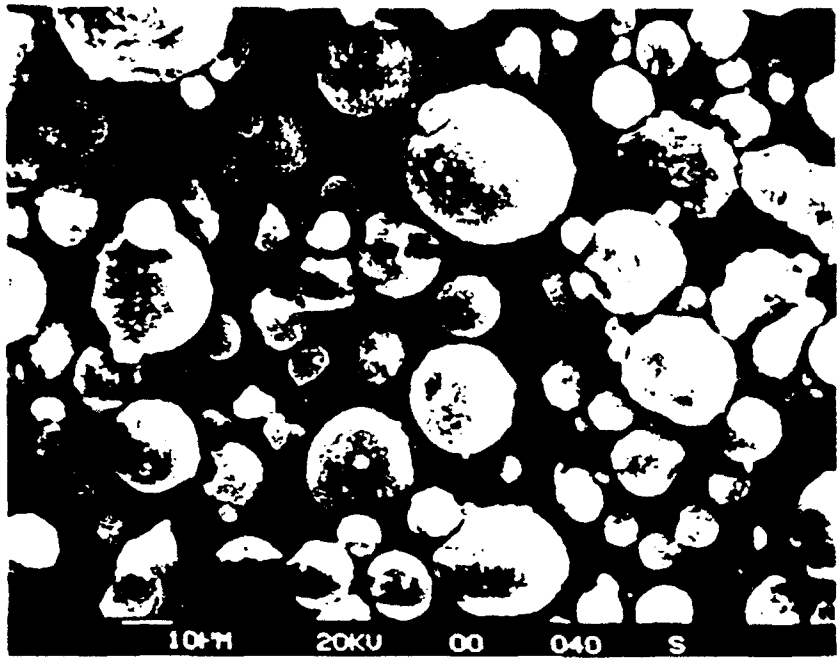

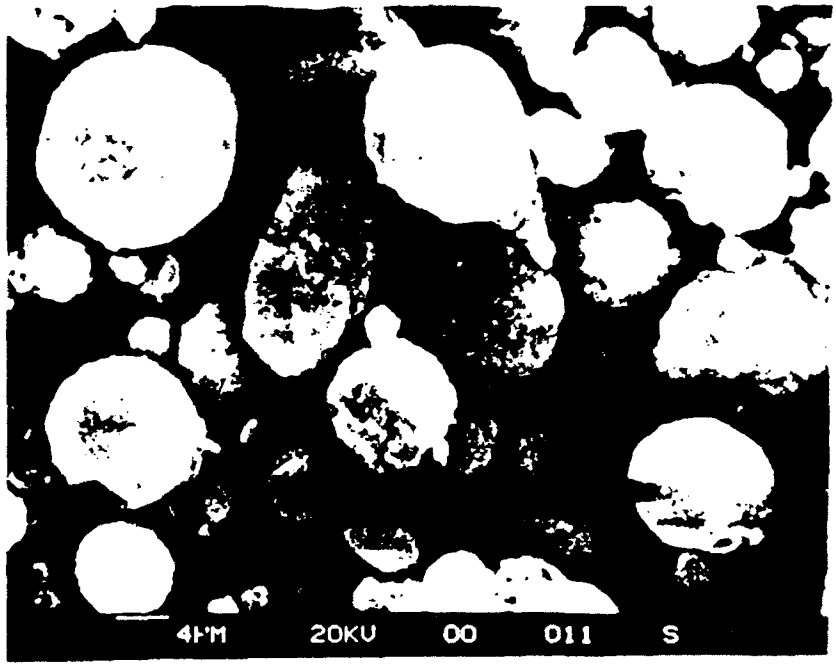

(b)

Fig. 1

(a)

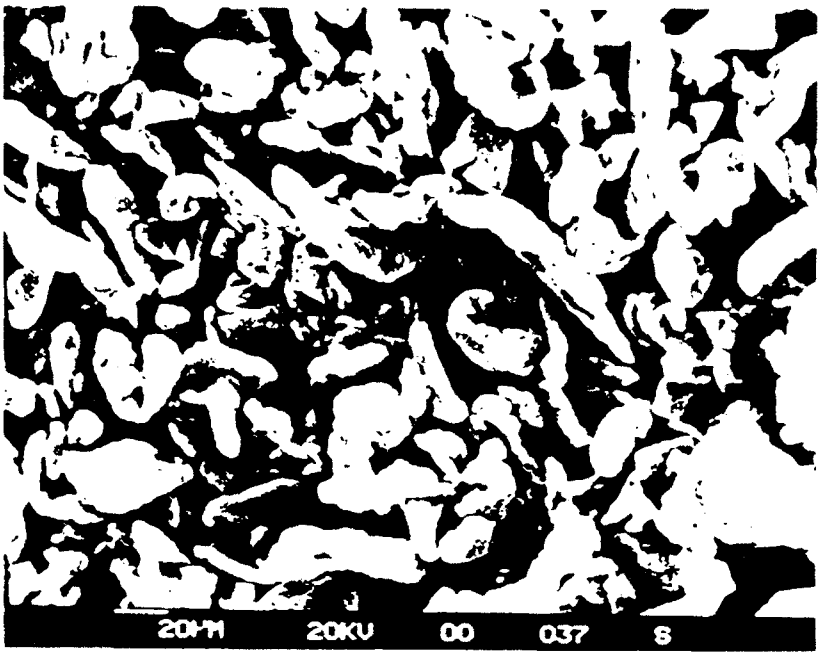

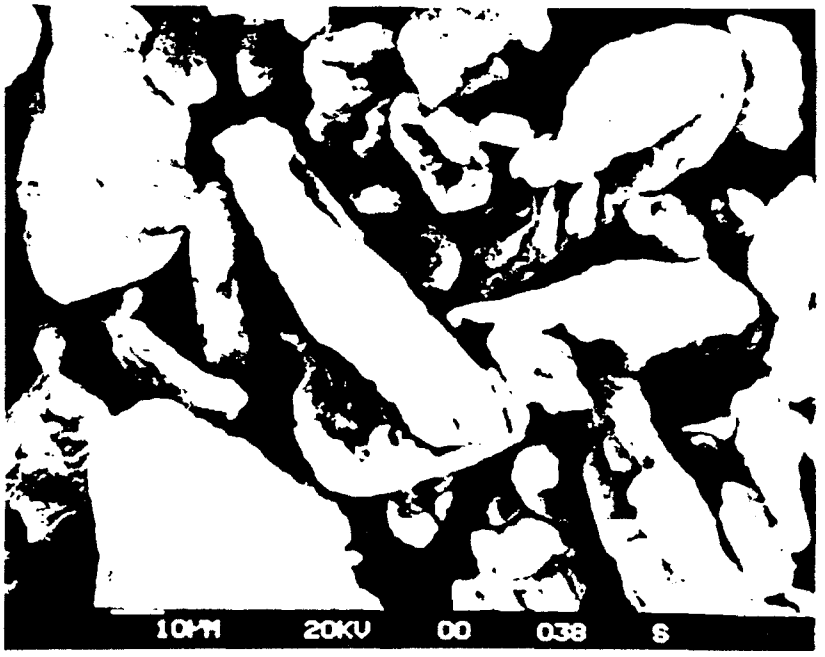

(b)

Fig. 2

(a)

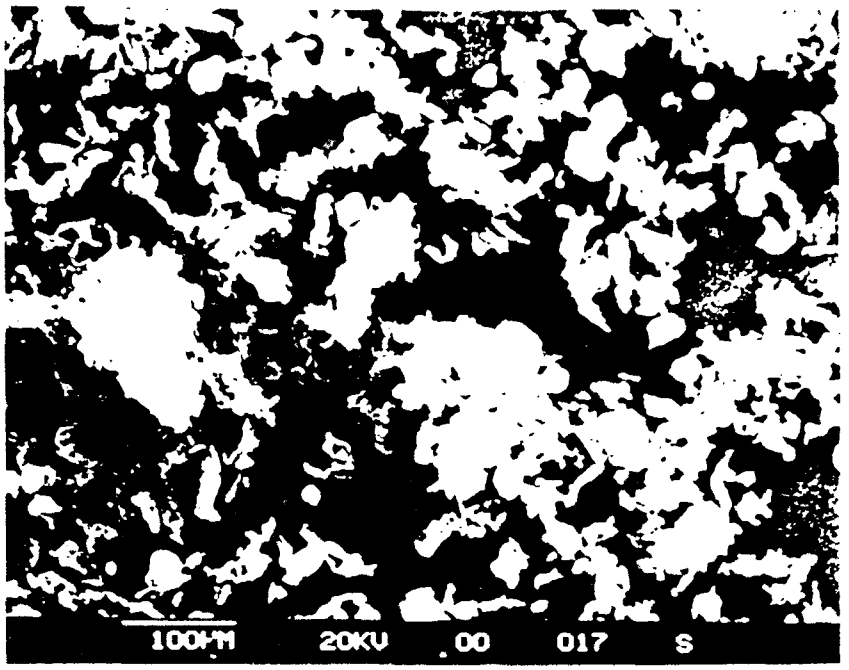

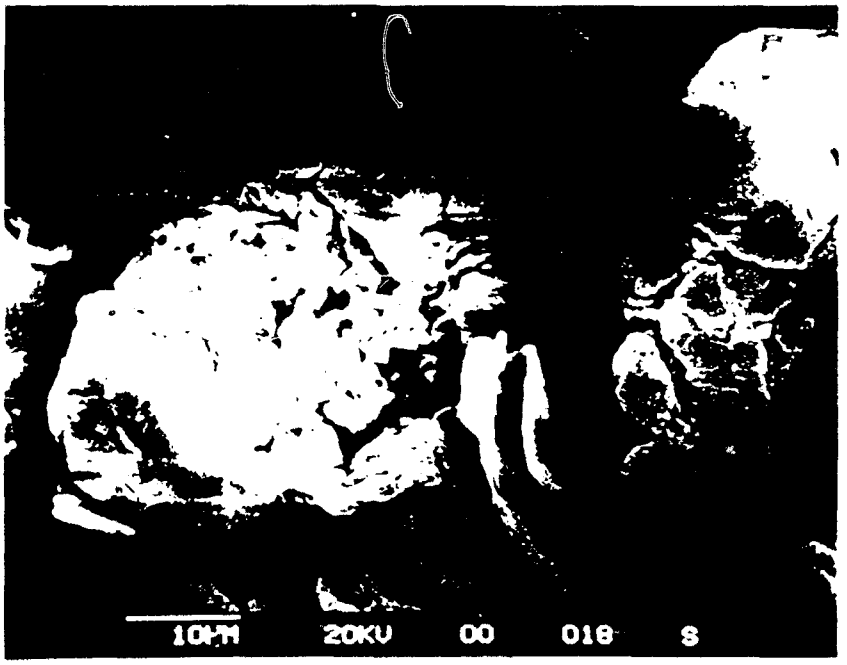

(b)

Fig. 3

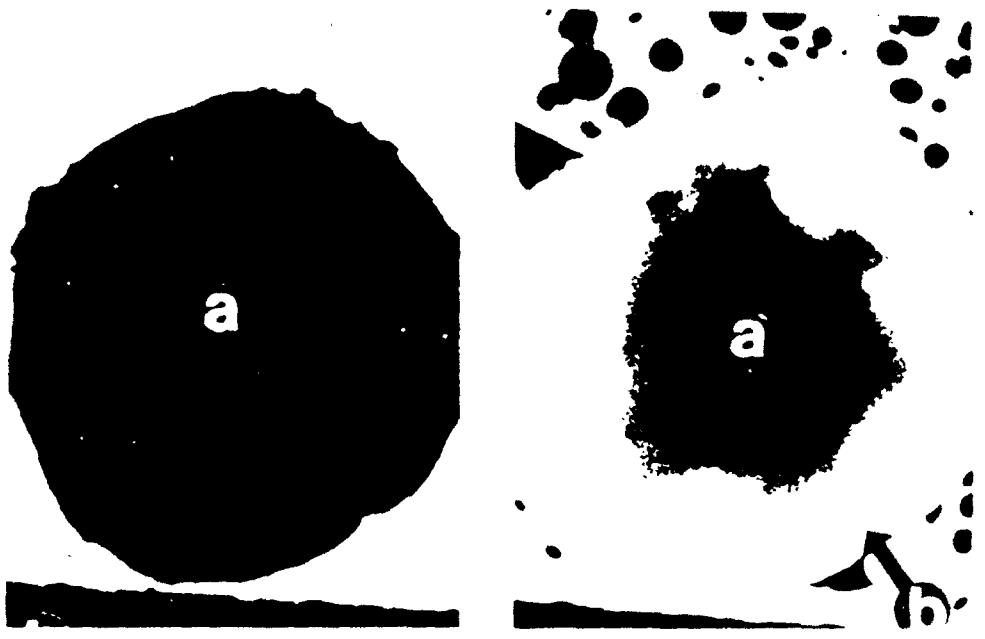

(a) (b)

Fig. 4

Fig. 5

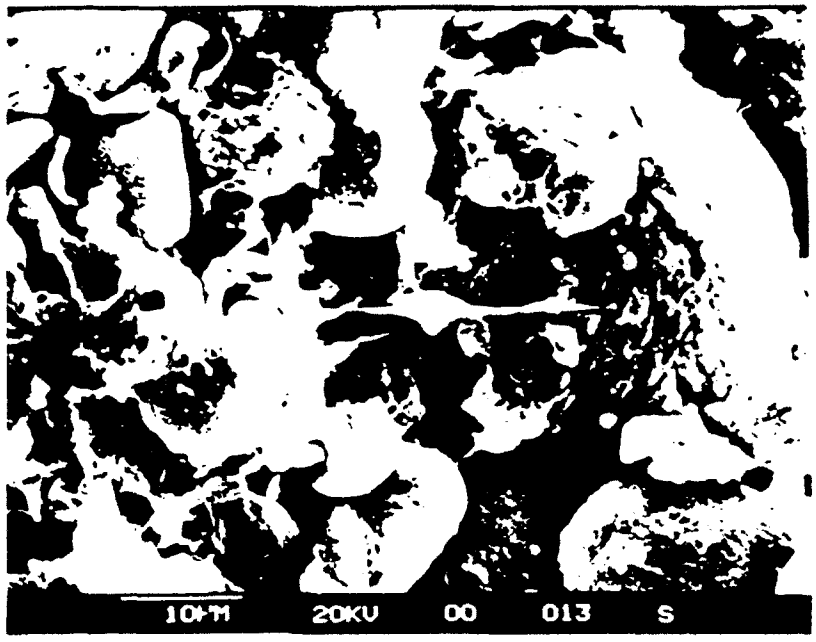

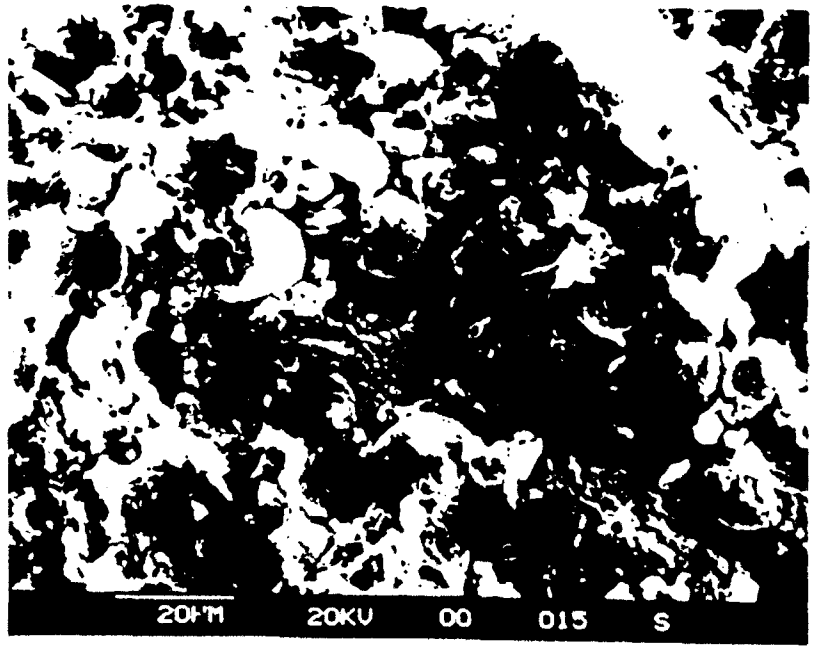

Fig. 6

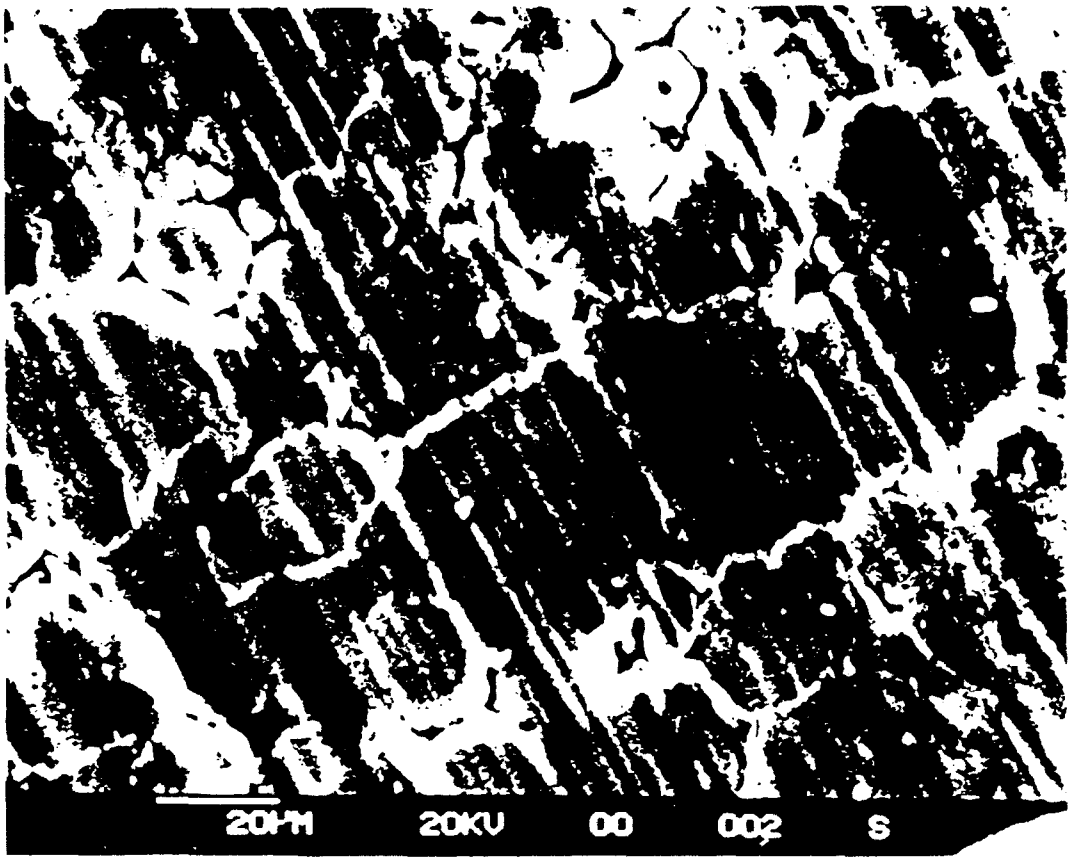

Fig. 7

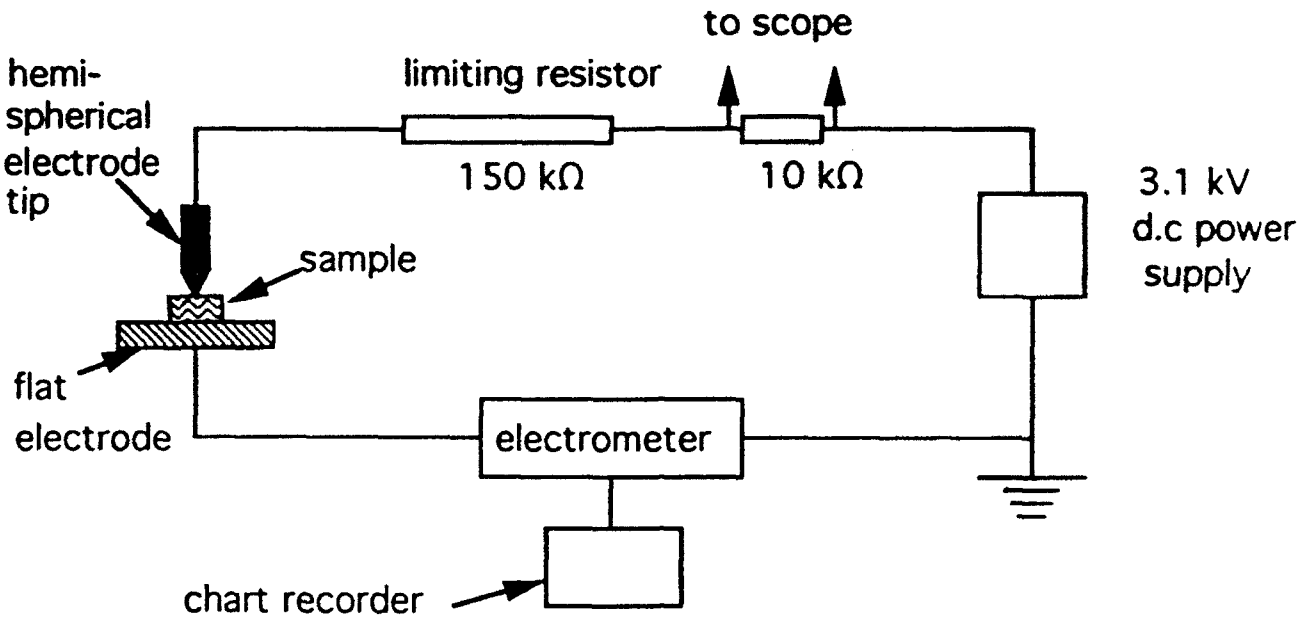
to scope
hemi-
spherical
electrode
tip
limiting resistor
150 kΩ
10 kΩ
3.1 kV
d.c power
supply
sample
flat
electrode
electrometer
chart recorder

Fig. 8

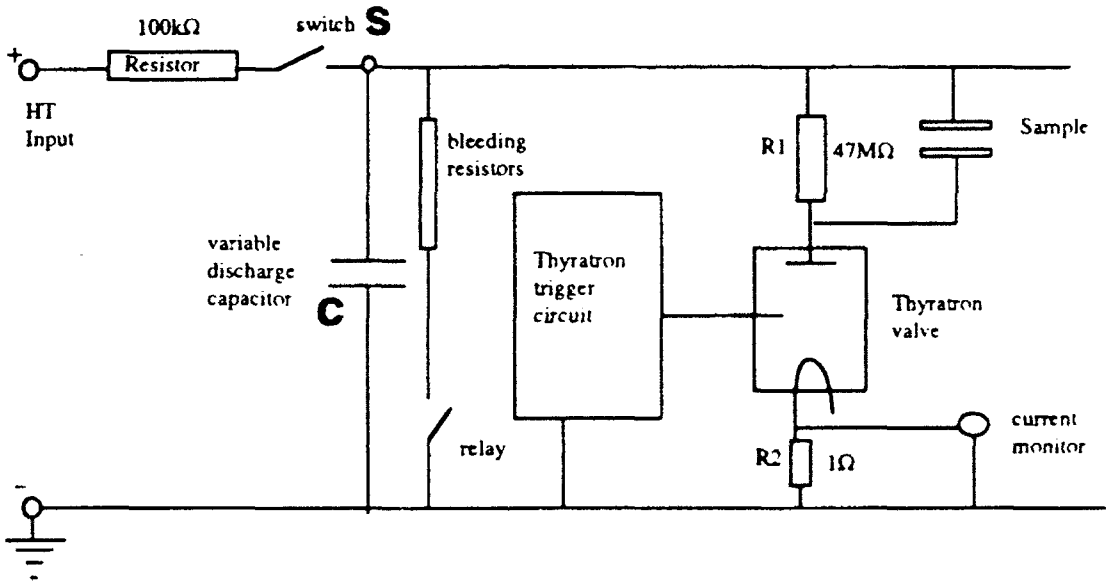
100kΩ
switch S
Resistor
HT
Input
bleeding
resistors
R1
47MΩ
Sample
variable
discharge
capacitor
C
Thyratron
trigger
circuit
Thyratron
valve
relay
current
monitor
R2
1Ω

Fig. 9

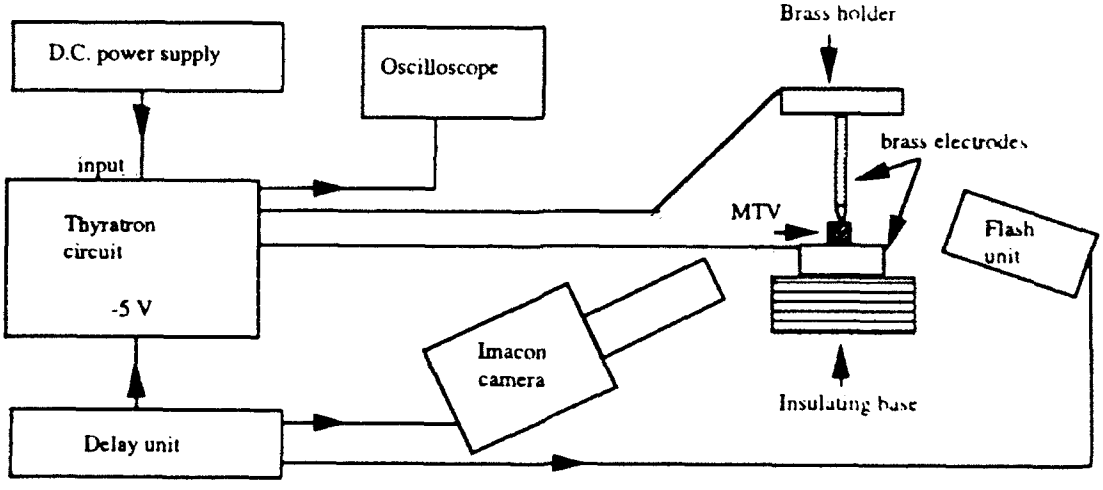
D.C. power supply
Oscilloscope
Brass holder
input
brass electrodes
Thyratron
circuit
-5 V
MTV
Flash
unit
Imacon
camera
Insulating base
Delay unit

Fig. 10

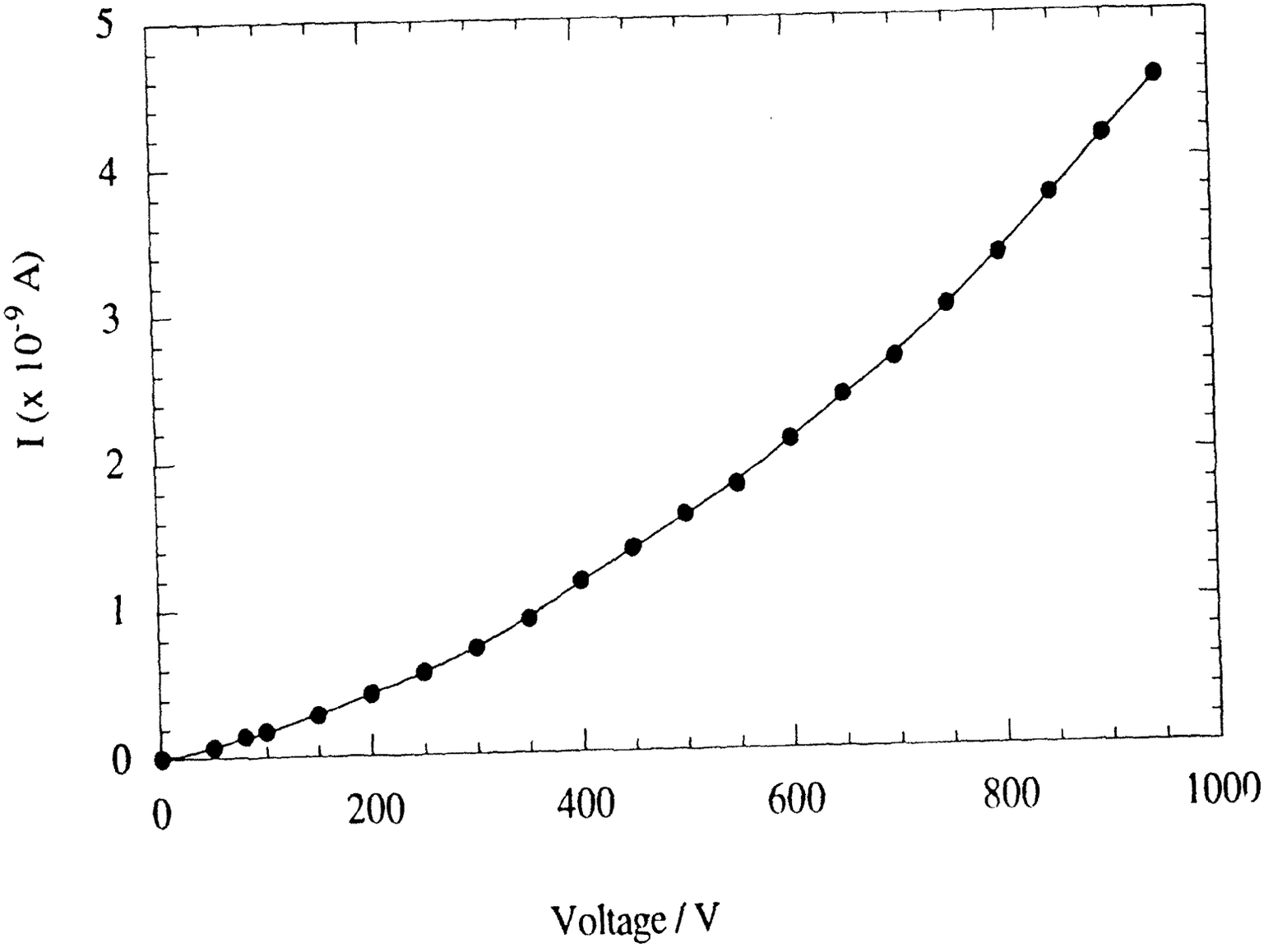

Fig. 11

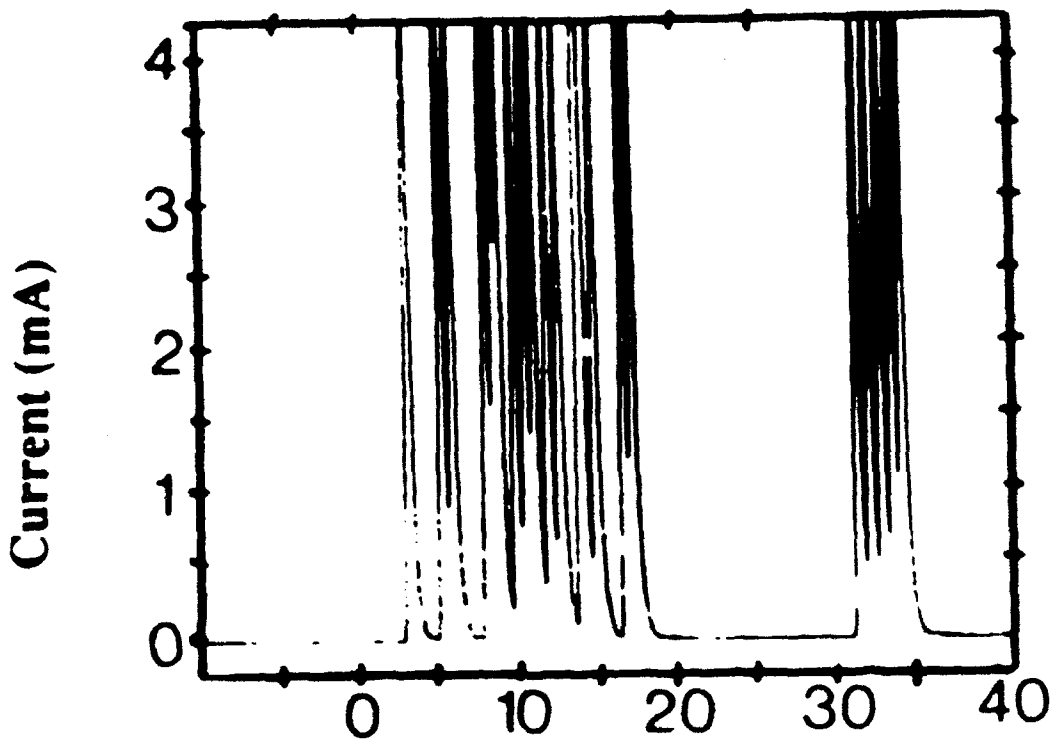

Fig. 12

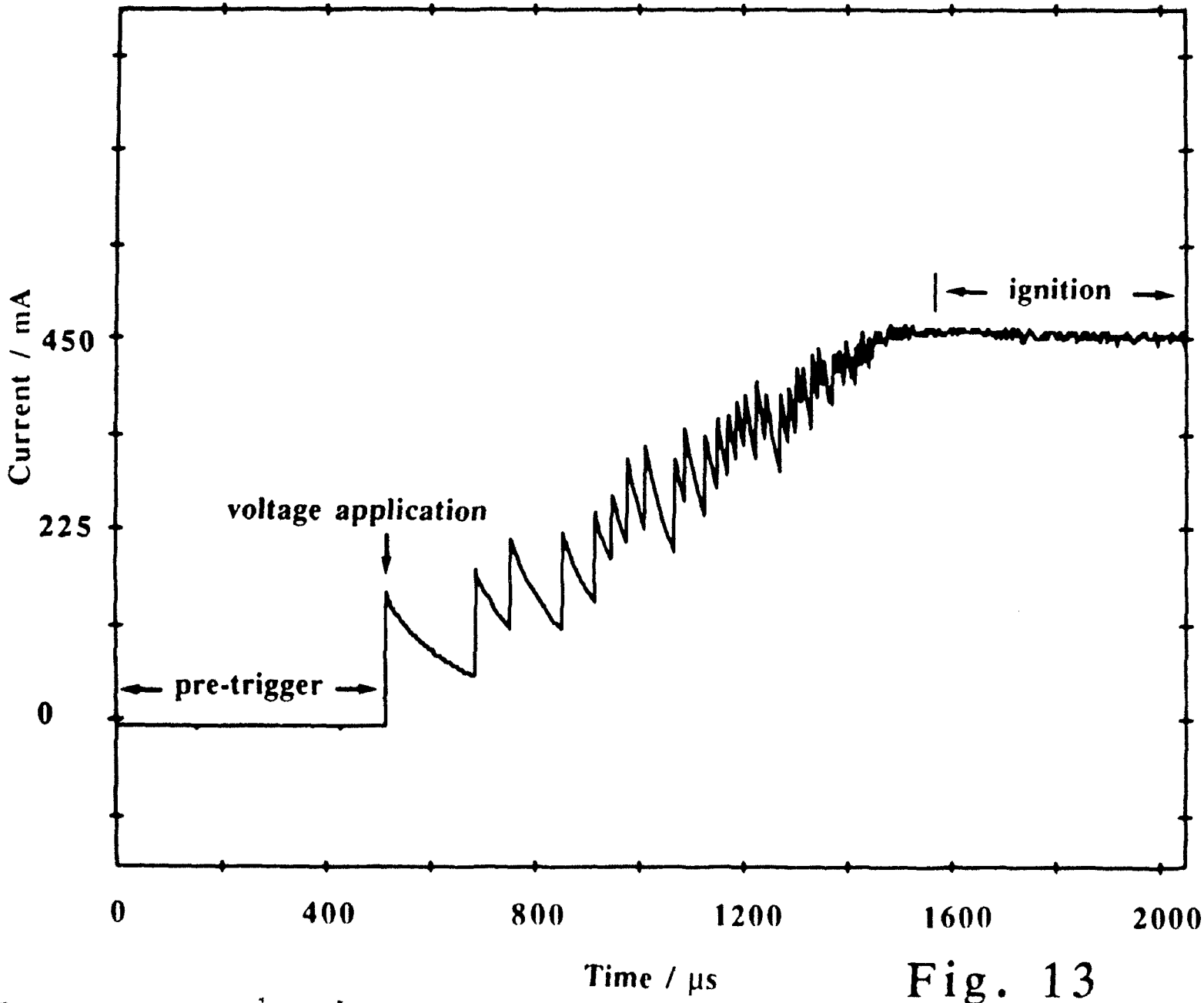
Current / mA
450
225
0
ignition
voltage application
pre-trigger
0
400
800
1200
1600
2000
Time / μs

Fig. 13

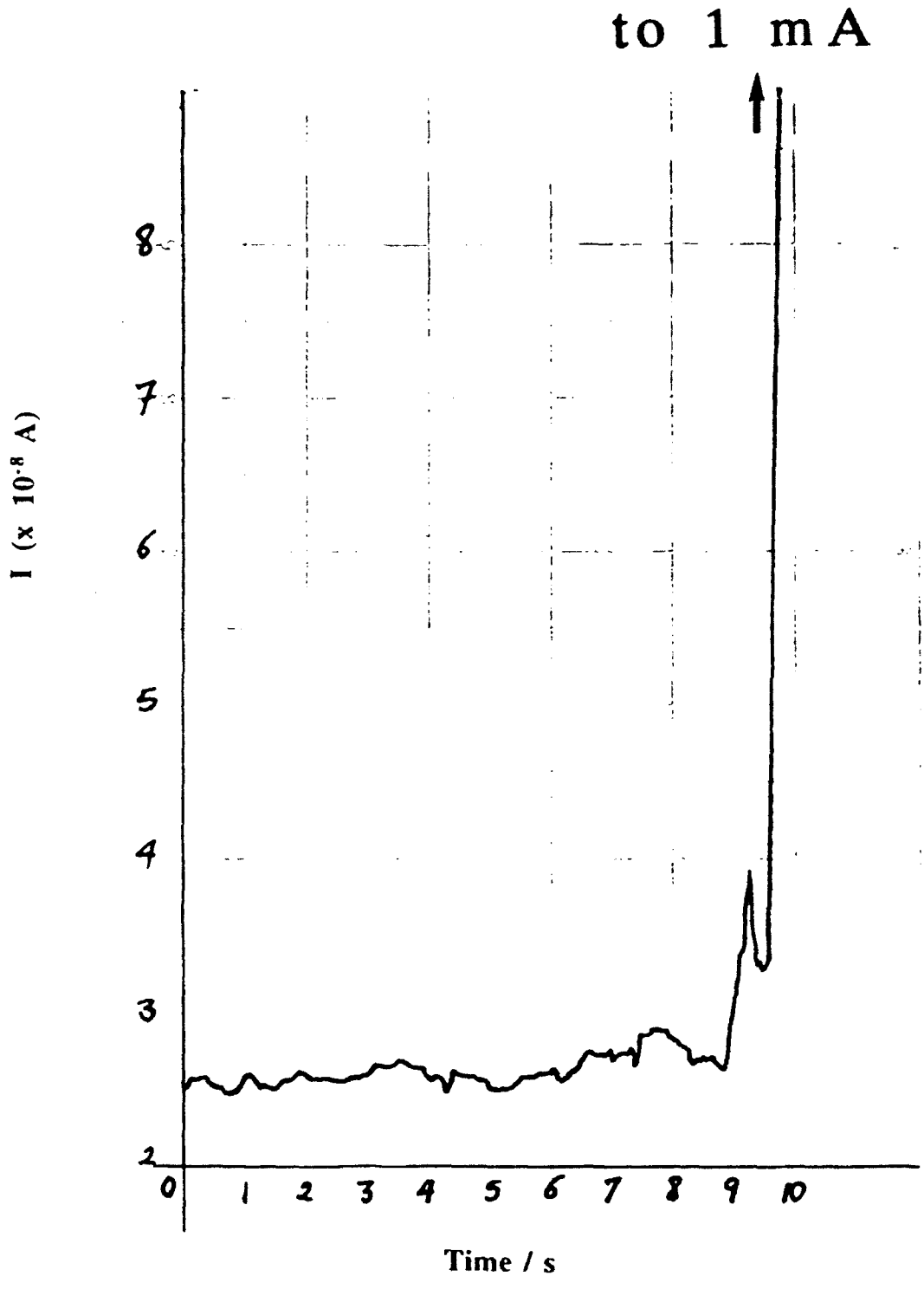

Fig. 14

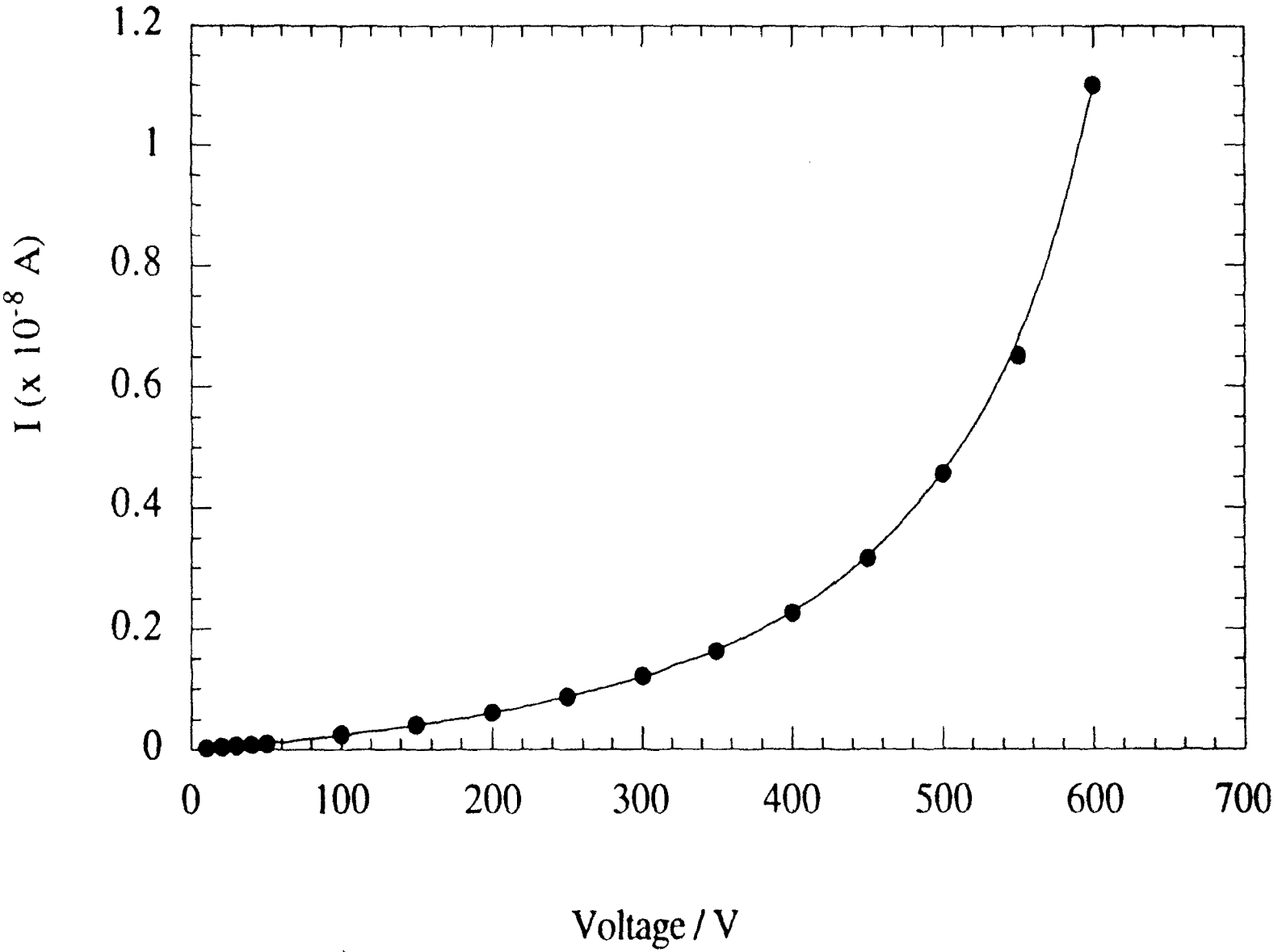

Fig. 15

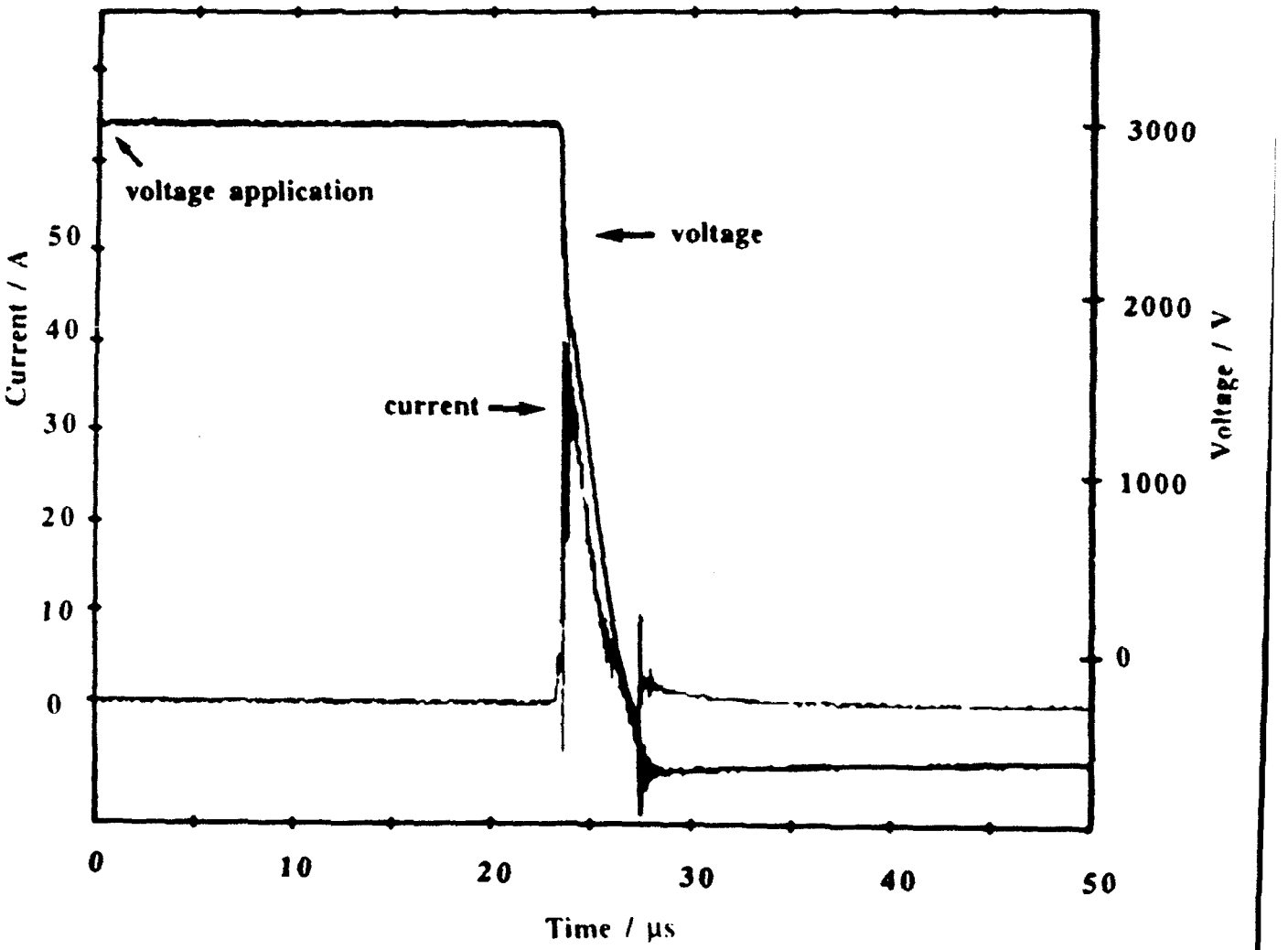
voltage application
voltage
current
Current / A
Voltage / V
Time / μs
0
10
20
30
40
50
0
1000
2000
3000

Fig.16

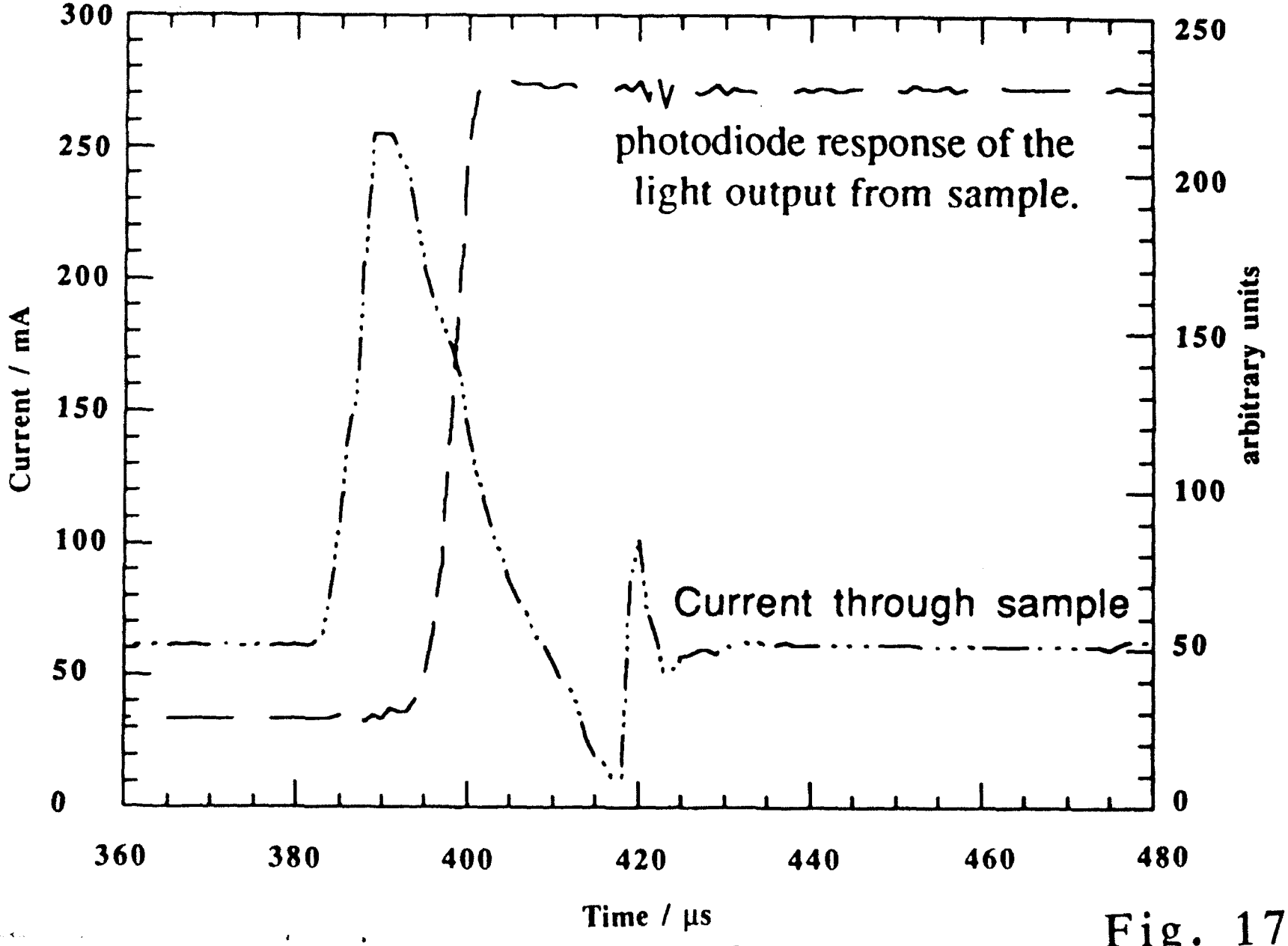
300
250
200
150
100
50
0
Current / mA
250
200
150
100
50
0
arbitrary units
photodiode response of the
light output from sample.
Current through sample
360
380
400
420
440
460
480
Time / µs

Fig. 17

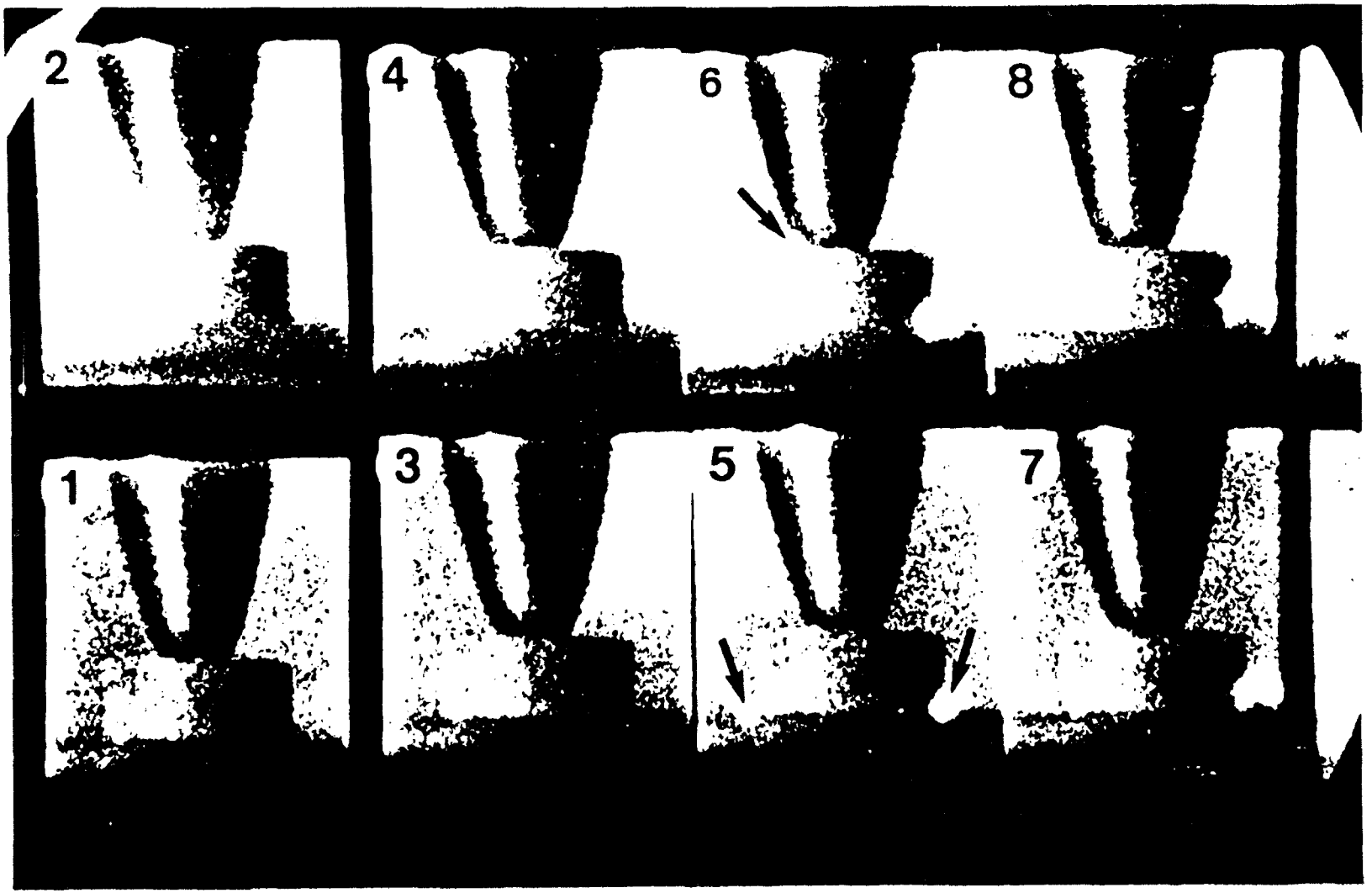

Fig. 18

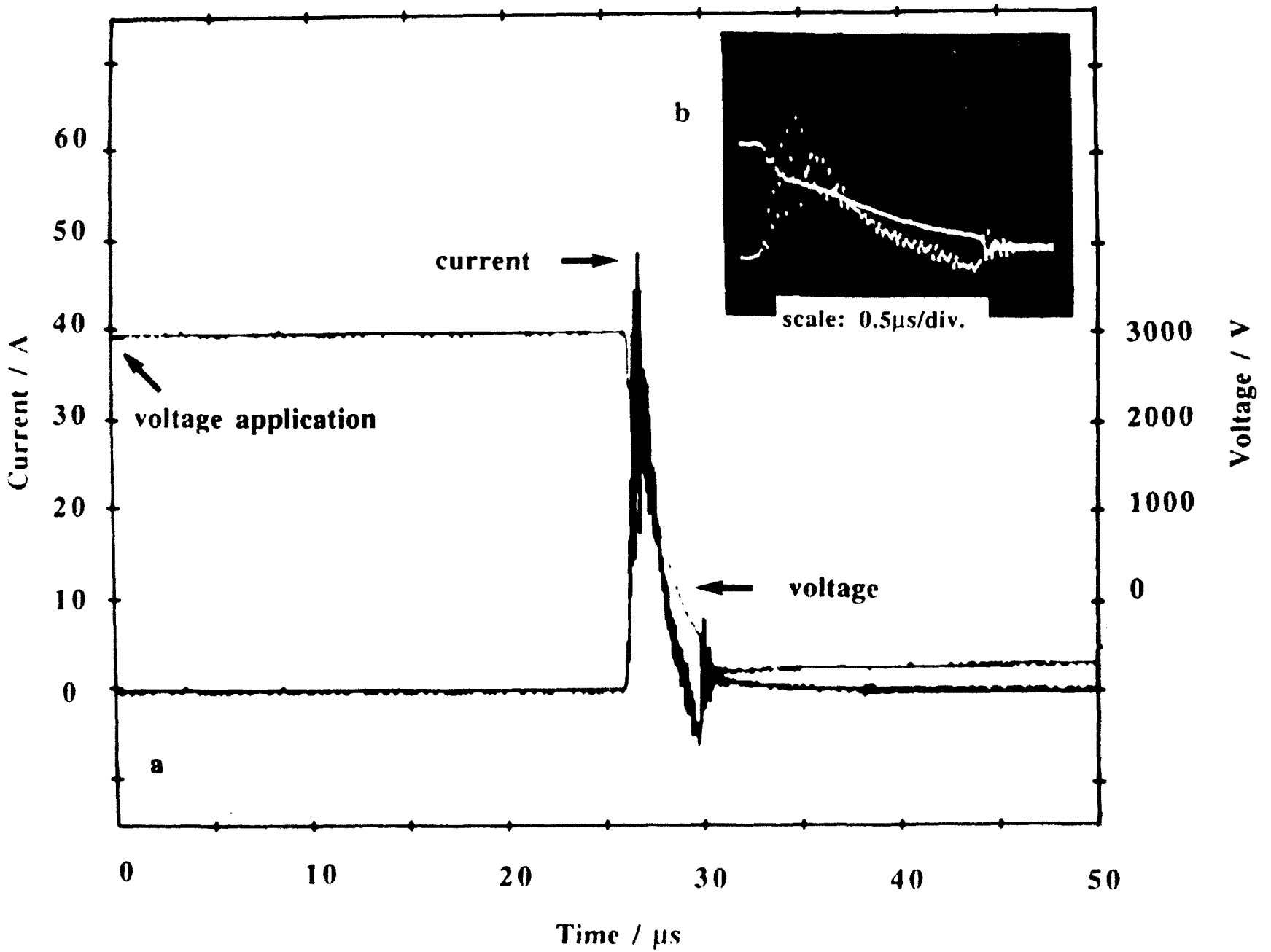
b
current
scale: 0.5μs/div.
voltage application
voltage
a
Current / A
Voltage / V
Time / μs
0
10
20
30
40
50
60
0
1000
2000
3000

Fig. 19

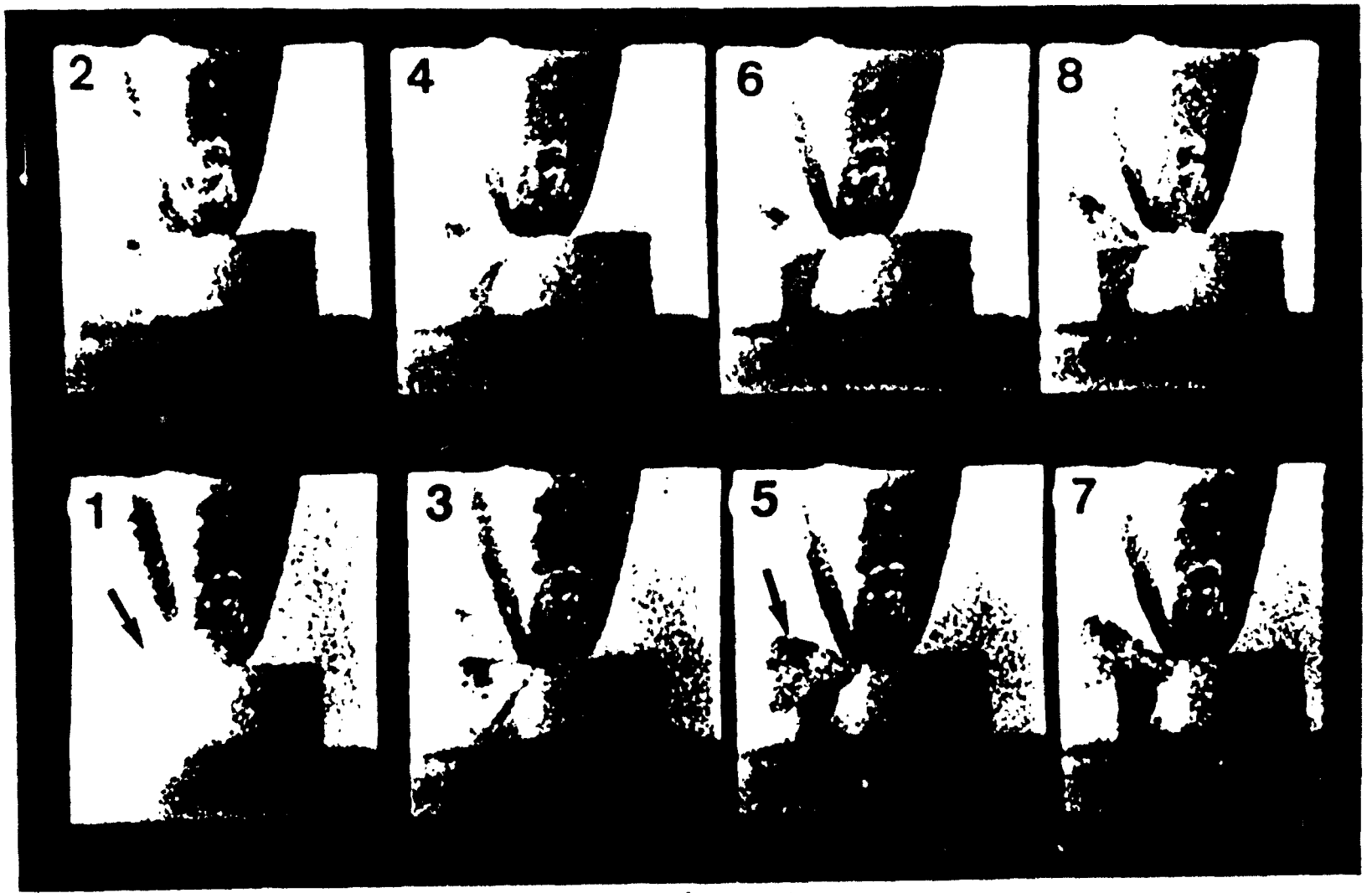

Fig. 20

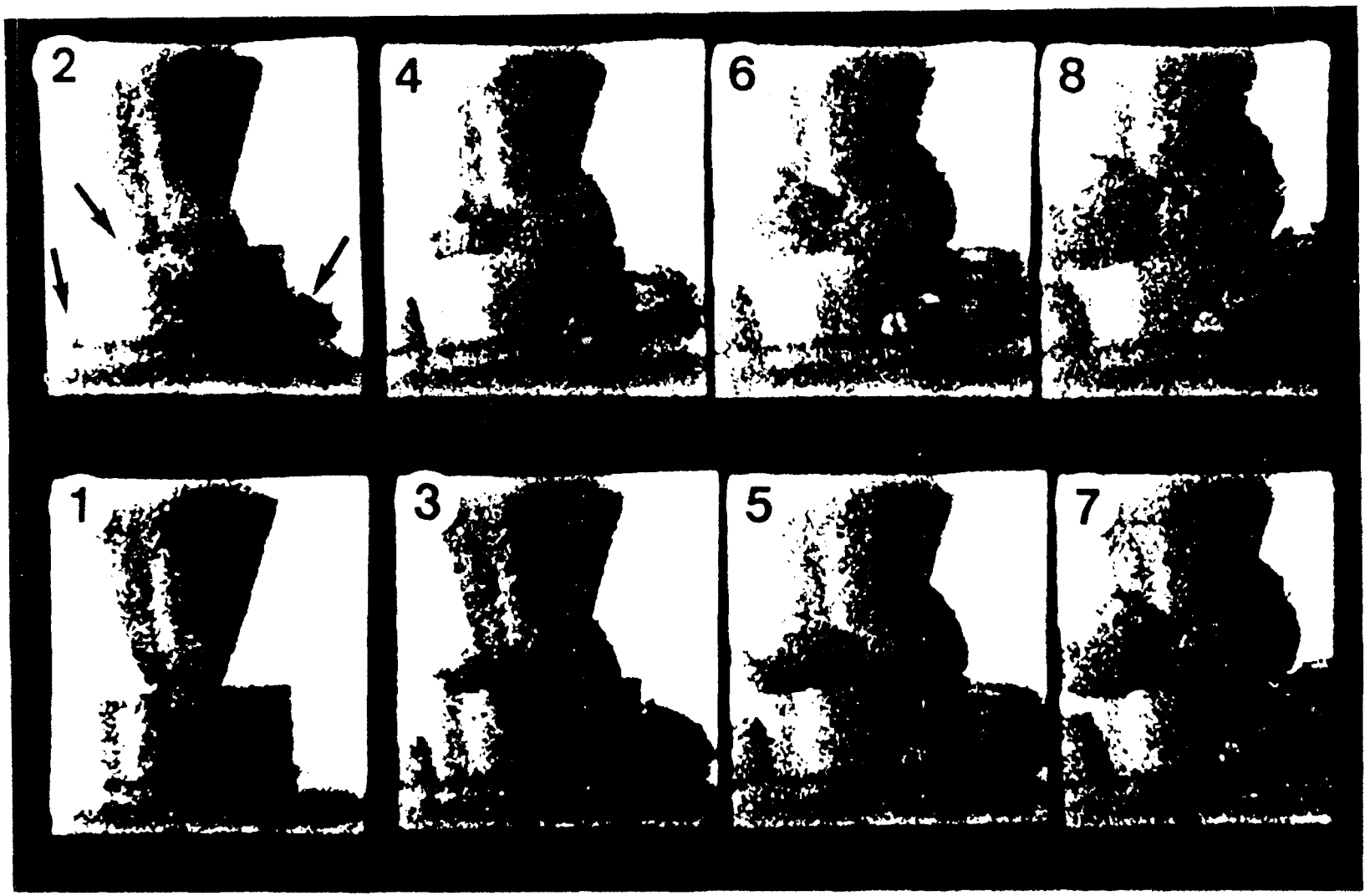

Fig. 21

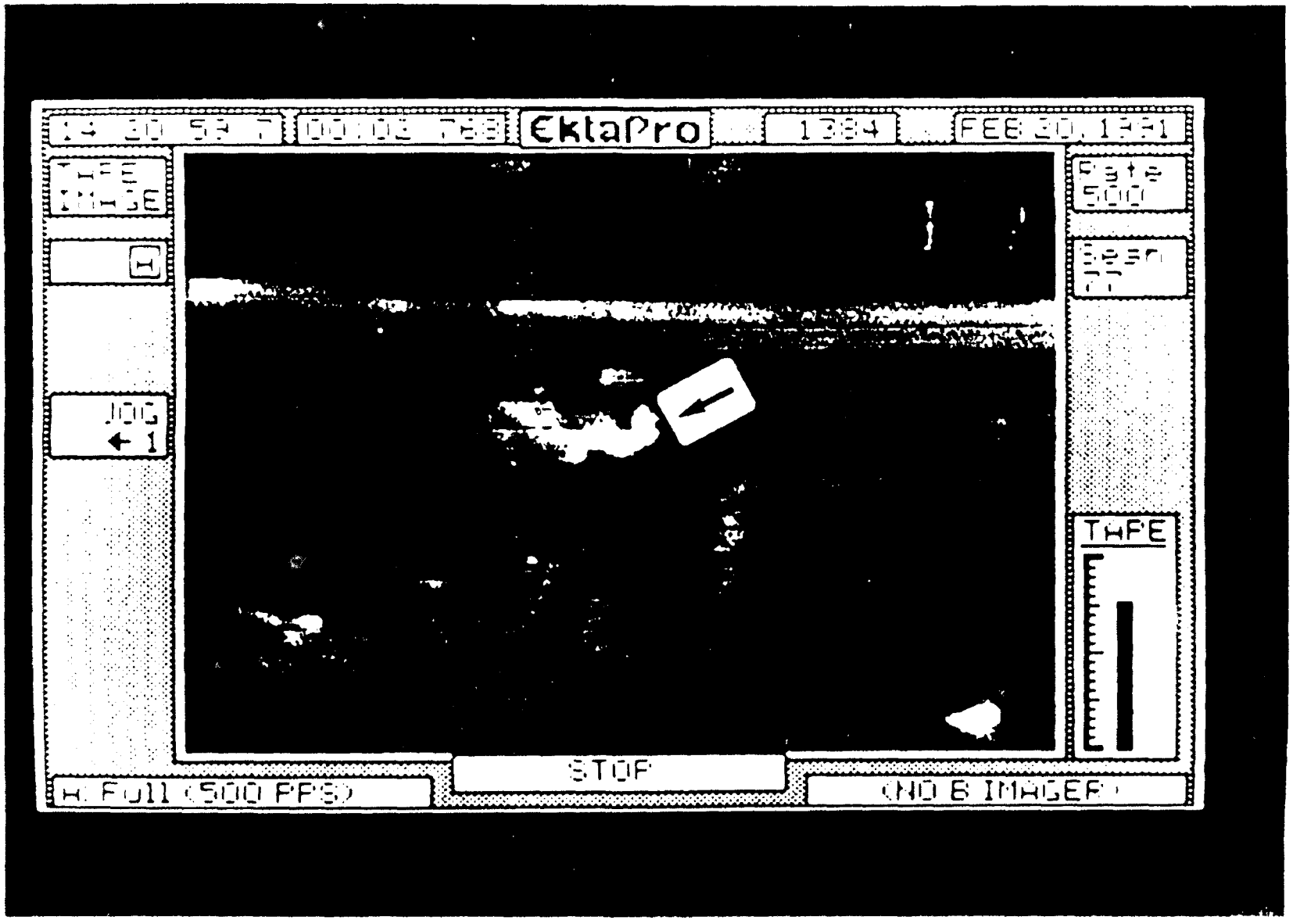

Fig. 22

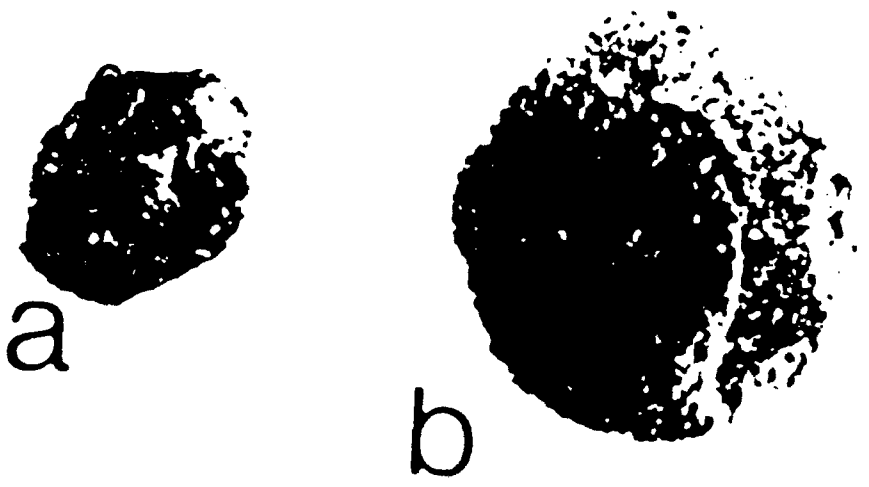

Fig. 23

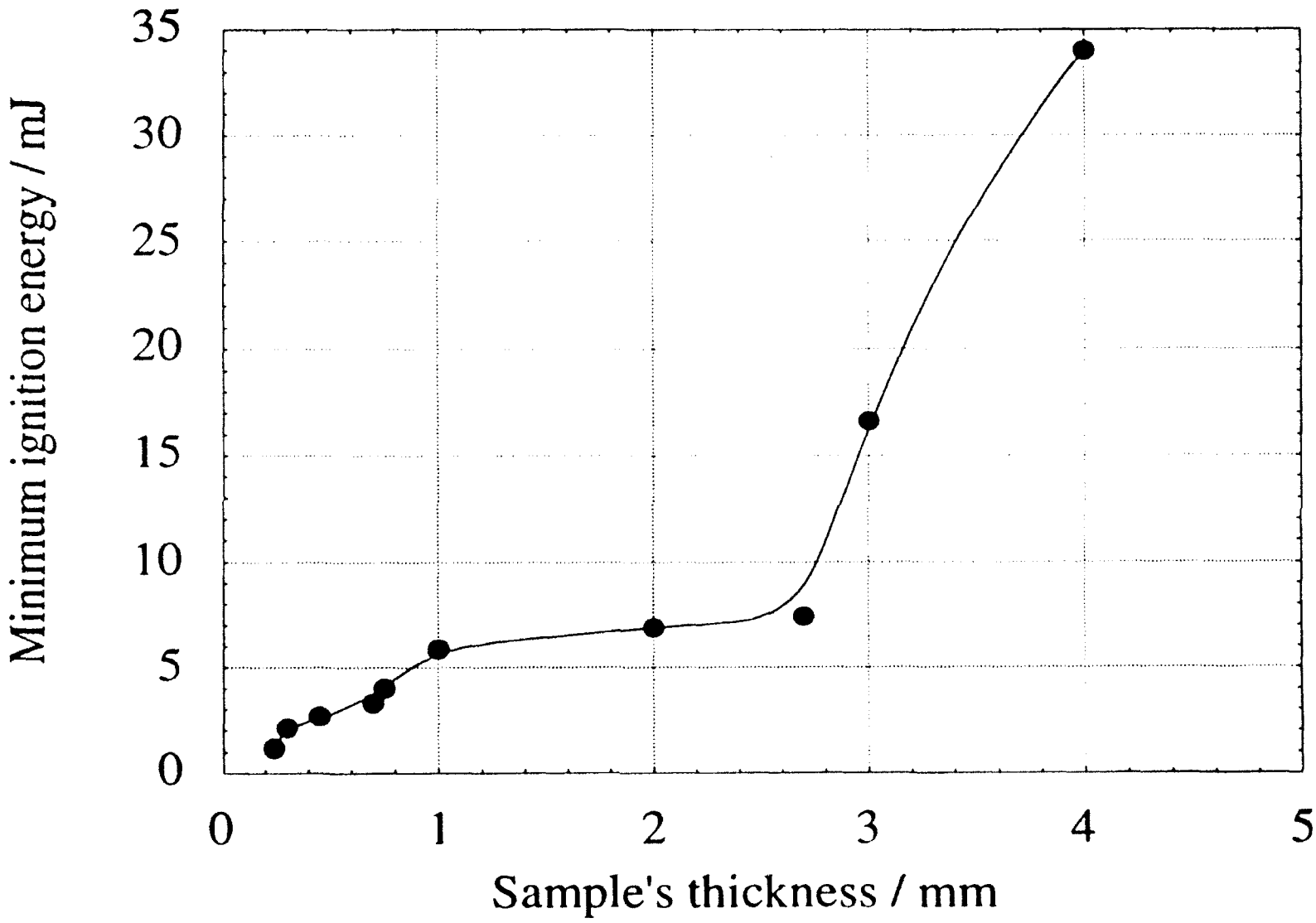
Minimum ignition energy / mJ
35
30
25
20
15
10
5
0
0
1
2
3
4
5
Sample's thickness / mm

Fig. 24

a

b

Fig. 25

Low Energy Laser Ignition of Magnesium-Teflon-Viton Compositions

1. Introduction

Magnesium-Teflon-Viton (MTV) compositions are made of viton-coated magnesium and teflon particles. When heated to high temperatures, chemical degradation and reaction between the various ingredients of the compositions occur. The main exothermic reaction is between the Mg and the fluorine of the polymers, giving MgF_2. At sufficiently high temperatures, the exothermicity leads to self-heating and ignition. Moreover, the ignition is self-sustained and high temperatures are generated. Thus these compositions can be useful in a number of ways, particularly as igniters. The compositions are often used in a pellet form, which is produced by compacting the loose composition in specially constructed metallic dies. During the last 10 15 years a number of unexplained ignitions of the compositions during compaction and pellet-ejection stages, and handling has been reported by Dierks (1986) and by Potter (1988). It has been suggested by Haq and Chaudhri (1989) that MTV pellets may suffer electrical breakdown as a result of the accumulation of electrostatic charges on them during compaction, which may lead to their dielectric breakdown and accidental ignitions.

To examine this further, more work has been carried out in this laboratory by studying the dielectric breakdown and consequent ignition of MTV pellets by electrical means. It has been shown that the dielectric breakdown of a pellet does indeed cause its ignition, the minimum electrical energy required for the breakdown and subsequent ignition is approximately 6 mJ (details to be published later) and the time delay following the breakdown to ignition is in the range 20 æ32 µs.

The laser has been used extensively for testing the ignition behaviour of propellants, explosives and pyrotechnics by Holy and Girmann (1988). The ignition thresholds for Mg/teflon and other compositions were measured by these workers as a function of sample chamber gas pressure by irradiating the test samples with focused pulses from an argon ion laser of wavelength of 514.5 nm. The Mg/teflon composition was found to have decreasing thresholds with increasing chamber gas pressure and decreasing pellet density. In the case of a 65 µm spot diameter of the laser beam and a pulse duration of 20 ms, the threshold

increasing chamber gas pressure and decreasing pellet density. In the case of a 65 μm spot diameter of the laser beam and a pulse duration of 20 ms, the threshold energy values were found to be in the range of 5.6 æ 32 mJ, corresponding to incident energy densities of 1750–9640 mJ mm^{-2}. No information was given about the delay time between irradiation and ignition.

Unfocused low energy Q-switched and non-Q-switched ruby laser irradiation of individual single crystals of ß-lead azide has been studied using high-speed photography (Hagan and Chaudhri, 1981). It was found that the initiation of a fast reaction occurred at isolated sites, which were probably defects and acted as absorption centres in the dielectric crystals which were otherwise transparent to the ruby laser wavelength of 694.3 nm. They argued that it was the power and not the energy of the incident beam that controlled the initiation of ignition behaviour under these low energy irradiation conditions. A thermal mechanism of ignition was suggested, based on the variation of the time delay to initiation of ignition with the incident laser energy.

Laser initiation of ignition in pyrotechnics using a CO_2 laser (l=10.6 μm) has also been carried out by Oestmark (1985) and by De Yong and Valenta (1989). Oestmark et al (1985) used the laser to heat a pyrotechnic mixture of Mg and $NaNO_3$ with various pulse widths, and it was concluded that the laser ignition technique was useful for the calibration of conventional sensitivity tests as well as for risk analyses in practical situations. De Yong et al (1989) measured the time delay to ignition of MTV pellets as a function of the incident radiation flux, composition density , formulation (e.g.,pressed powder, and extruded pellets) and the physical form of the sample. The incident laser beam was perpendicular to the sample face. It was shown that as the flux increased, the time delay to ignition decreased;the time delays were 30 æ 35 and 220 æ 500 ms for flux values of 400 and 75 Wcm^{-2}, respectively. All the MTV samples showed erratic build-up to ignition before sustained combustion ensued. They suggested that several reactive sites formed on the sample surface before ignition and self-sustained combustion took place. It was also noted by Habersat (1981) that when MTV samples were irradiated with the laser beam, there was often a rapid change in the intensity of the visible light emitted by the samples before steady state combustion commenced.

In the light of the above, it appears that ignition may initiate at localized sites. In order to examine this further and to measure the minimum laser energy for ignition, we decided to carry out ignition studies of our MTV compositions

using high-speed photography working at framing rates of up to 500,000 frames per second. In the work reported below, it is shown that the self-sustained fast reaction does indeed initiate at microscopic regions.

2. Experimental

All laser ignition experiments were performed on unconfined pellets of three types of magnesium-teflon-viton (MTV) composition, designated as types 1, 2 and 3. The pellets were 5 mm in diameter and 1, 2, 3, 4 and 5 mm in thickness. The distributions of Mg particles (size in the range of submicrometre to several micrometre) were different in the three types, with the average particle size in the compositions being in the order 1 > 2 > 3. The pellets were obtained from RARDE, Fort Halstead and they were from two different batches, namely A & B. The laser employed was a Nd/Glass (system 2000, J. K. Lasers Limited, Rugby, England). The laser beam was unpolarised and its wavelength was 1060 nm; in the non-Q-switched mode, the pulse duration was 560 μs. The laser output energy was measured with a laser calorimeter (ITL, model 136) and it was found that the output energy was produced fairly reproducibly (i.e., variation of less than 5% from one shot to another) for a given applied voltage on the flash lamp capacitors. The beam diameter was 13 mm and the output energy could be varied in the range of 1.5 to 10 J by altering the voltage on the capacitors energising the flash lamp; very occasionally, the laser was overdriven to produce an output energy of 11.5 J. A typical temporal profile of the laser pulse is shown in figure 1. This was taken by passing the laser beam through a filter (Schott glass type RG780), which transmitted only above 780 nm, reflecting it off a microscope slide placed at 45^{O} to it, allowing it to fall on a fast photodiode (type BPX 65), and recording the signal on an oscilloscope (Gould digital storage type 4035). The sync. pulse from the control unit is also displayed in the figure . The duration of the laser pulse for a beam energy of 10 J was 560 μs. At this output energy the lasing action coincided quite reproducibly with the falling edge of the sync.pulse, as shown in the figure. The output energy distribution across a diameter of the beam was determined by placing a 1 mm diameter aperture between the laser and the calorimeter. The energy of the emergent beam was then measured at 20 - 25 aperture positions along the diameter. Thus the energy distribution across a diameter of the beam was found to be reasonably uniform (Ramaswamy, A. L., private communication 1991).

Three types of experimental arrangement were used and in only two of them high-speed photography was employed. In one (see figure 2), the sample was placed on a sheet of black paper using a piece of double sided adhesive tape. This assembly was then stuck to a concrete block, 150 mm in thickness, and the sample surface placed at an angle of 45^{o} to the laser beam. The laser beam passed through a 3 mm diameter slit in a steel plate of 1mm thickness, as shown. The damage/ignition resulting from the laser irradiation was photographed at framing rates of up to 10,000 frames per second with a rotating prism camera (HySpeed H10/16;John Hadland Photographic Instrumentations Ltd, UK) using external light from a continuous light source, as shown. The synchronization was achieved manually by switching on the camera first, then firing the laser immediately (i.e; within a fraction of a second).

The event was recorded on black & white film(type:Ilford HP5, 400 A.S.A.). With this arrangement the entire process of ignition and its propagation, which lasted approximately 0.6 s, could be photographed. However, the framing speed of the camera was inadequate for accurately measuring the time delay between the irradiation and the initiation of ignition. In the second arrangement (see figure 3), the slit was placed on the exit end of the laser and a fast (0.5–1 ns) photodiode (type BPX 65), was placed at about 100 mm from the test sample. The spectral response of the photodiode was in the wavelength range of 400–1000 nm and its peak sensitivity was at 850 nm. A Schott glass filter (type KG1), having transmission between (250 – 930 nm) was placed in front of the photodiode to filter out the reflected laser beam. The ignition was detected with the photodiode, and the signal recorded on an oscilloscope. With this arrangement, it was possible to determine an approximate value of the time delay (see figure 4) between the impact of the laser beam on the sample and the resulting ignition. For a total beam energy of 0.52 J incident on the sample, this time delay was estimated to be about 30 μs or shorter. This uncertainty in measuring the time delay was caused by the reflection of the laser pulse from the sample surface and even when there was no ignition from the sample, a strong signal, corresponding to the reflection of the laser pulse, appeared. In the third arrangement, shown in figure 5, an image converter framing camera (Imacon 790), working at up to 500,000 frames per second, was used. Again the unfocused laser beam passed through a 3 mm diameter slit in a steel plate of thickness of 1 mm, which was placed on the exit end of the laser window, and the beam impacted the test sample placed at an angle of 45^{o}. A gelatin filter (Transmission: 460–690 nm) was placed in front of the camera objective lens to block off any

reflected infra-red beam, from entering the camera. The irradiation and ignition processes were photographed in reflection using the light from an electronic flash tube (Bowens Mono 400 D). The latter produced a peak intensity in the visible part of the spectrum after about 700 μs of being triggered. It was decided to trigger the laser and the camera from the original trigger signal of the flash tube, by using a dual pulse unit (Hadland Photonics) and a secondary delay unit (type JH-TDG. XLD10. John Hadland Ltd, England). In order to be able to photograph an ignition event, the laser and the camera were thus required to be triggered at 700 μs after the triggering of the flash tube.The dual pulse delay unit was triggered by manually shorting a circuit in the dual pulse unit, from which two simultaneous pulses were produced. One triggered the flash tube and the other actuated the secondary delay unit. The latter produced two pulses at selected times. One pulse triggered the laser control unit after a delay of 555 μs and the other one triggered the camera after 700 μs of the firing of the flash tube. These time settings allowed us to ensure that the laser pulse, the first frame of the camera, and the peak intensity of the flash tube coincided in time. Using the arrangement shown in figure (3), some preliminary experiments were conducted to determine the laser energy required for causing ignition of the MTV samples. If the slit diameter was reduced to 1 mm, no ignition occurred for an incident beam energy of 206 mJ (52.2 mJ mm^{-2}), even if the same sample area was irradiated 3 or 4 times (the time duration between two consecutive irradiations was ~ 3 min). However, when the slit diameter was increased to 3 mm, all samples (from batch A) ignited at the 2nd, 3rd or 4th impact by the laser pulse. On the other hand, if the incident laser energy density was increased to 58.5 æ 61.2 mJ mm^{-2}, ignition of the different MTV compositions occurred at the first irradiation. Samples (type 1 & 2 from batch B) were readily ignited for an incident laser energy of 0.52 J at the first laser shot while type 3 did not ignite. Therefore, in order to determine the minimum energy incident on the sample which could cause ignition, the delay time to ignition also needed to be measured. This was achieved using the third arrangement (figure 5) and this energy value was determined from the various quantities, viz., the laser pulse duration, the delay setting in the delay unit and the frame number of the photographic sequence in which the ignition occurred. By integrating the laser energy incident on the sample up to the ignition time, and taking into consideration the percentage of the laser light reflected from sample's surface, the minimum critical energy absorbed was determined. In some cases, if the laser irradiation did not cause the test sample's ignition, its surface was examined by SEM. To carry out this, a 20 nm gold film was sputter- deposited on the sample surface.

In order to calculate the percentage of the laser energy reflected from the sample surface, the refractive index of MTV samples should be known. Using the formula given by Shin et al (1989) for a metal–polymer system, such as ours, we estimate that the refractive index of the MTV samples is ~2.5. Therefore the reflectivity of those samples for unpolarised laser beam incident at 45^{O} is about 20%.

In another series of experiments MTV pellets were ignited thermally by bringing them into contact with a hot plate (see figure 6) whose temperature was measured with a digital thermometer (Portec, type K, Portec Inst.Ltd.U.K) having an accuracy of $\pm 1^{O}C$. Also, the time delay between the moments of contact and ignition was measured. The sample was inserted in a teflon tube 30 mm in length and 6 mm in diameter so that part of the sample remained protruding from the tube. The protruding part of the sample was brought into contact with the hot plate and a slight pressure was applied to it in order to maintain a good thermal contact. The initiation of an ignition was accompanied by the emission of visible light. The time between the contact and the initiation of ignition was measured with a digital stop watch for different temperatures of the hot plate. The ignition temperature of a sample was determined by bringing it into contact with the hot plate heated to a predetermined temperature. If no ignition occurred within 120 s of the contact, the sample was removed and the plate temperature raised by 10 K. Another sample of the same type was then brought into contact with the plate and examined for ignition. In this manner the ignition temperatures of the MTV samples of types 1, 2 and 3 (batch A) were determined.

To estimate the temperature rise in a MTV pellet irradiated with the laser beam of a given energy, we also needed to know the value of the absorption coefficient of the sample at the laser wavelength. This was determined from the transmission spectra of the MTV samples of different thicknesses obtained using a Perkin Elmer 1- 9 spectrophotometer.

3. Results

Samples from the batch A yielded slightly different results from those from the batch B. In the case of the samples from the batch A, when the incident laser beam energy density was 52.2mJ mm^{-2}, it was found that, except very

occasionally (1 in 20), there was no ignition of the test sample at the first irradiation. However, for the same incident energy and for the same irradiated area of the sample, ignition usually occurred at the second or the third laser shot, and the entire sample was consumed. If there was no ignition, the irradiated area of the sample was found to be darkened, perhaps due to any chemical reaction. It is interesting to note that when a teflon pellet(i.e; no Mg particles in it) was irradiated with the same laser energy, there was no darkening of the irradiated area.The incident energy densities, which were able to cause the ignition of the MTV samples (batch A) (5mm diameter &4mm thick) at the first or subsequent irradiations on the same irradiated area, are given in Table 1. The table shows that the type-1 composition (batch A) is the most sensitive and that the type-3 (batch A) is the least sensitive. However, the difference in the values of the absorbed ignition energies was rather small. Moreover, the energy density required to cause an ignition at the 2nd, 3rd or the 4th shot is significantly smaller than that required for causing ignition at the first shot. The minimum energy densities for the samples from the batch B are given in table 2. It will be seen that the types 1 & 2 of batch B are slightly more sensitive than types 1 & 2 of batch A. It is interesting that types-1 and 2 (batch B) were ignited at the first laser irradiation (energy density 36.5 mJ mm^{-2}) while type 3 (batch B) could not be ignited at all for laser beam energy density of 36.5mJ mm^{-2}.

Microscopic examination of the surface of a sample, which was darkened but did not ignite by the laser irradiation, revealed that the darkening was heavily localized around the Mg particles. A typical SEM micrograph of a darkened sample (type 1, batch A) surface is shown in Figure 7. Burnt/ reacted polymer is seen at arrow (a); some Mg particles appeared to have been ejected from their sites due to the laser irradiation (see at arrow (b)). The arrows at (c), show a few coated Mg particles of the original composition.

We were able to obtain high-speed photographic sequences, using both types of camera. Figure 8, shows a sequence of selected photographs of an ignition of an MTV pellet (type-1, batch A). The laser beam impacts the sample (5mm in diameter & 3mm in thickness) in frame 1, which leads to the emission of a strong flash of light (see frames 2&3). After this initial flash, which lasted for about 300 μs, the intensity of the emitted light decreases a little, but the reaction front continues to propagate approximately uniformly at ~ 0.1 ms^{-1}. In frames 3,15,117,119 and 225, the ignition front is shown with arrows. It is interesting to note that just ahead of the ignition front, a dark band, about ~ 0.7 mm thick, appears (see, for example, frame 119). This band could be due to the partial

value of the time delay to ignition was obtained from the sequences taken with the Imacon camera working at an interframe time of 20 μs. Figure 9 shows a sequence of photographs of the laser irradiation on the same sample (type 3, batch A) area at the fourth instant; in this case the entire sample was consumed. From this sequence the time delay between the moment of irradiation and the initiation of an ignition can also be estimated approximately. The irradiation begins in frame 1 and in the next frame, the sample surface shows a luminous zone, which we interpret as the initiation of burning. We estimate that the delay time is 20 μs. From the knowledge that at an angle of incidence of 45^{o} about 20% of the incident energy is reflected from an MTV sample, the amount of incident laser energy which is actually absorbed by the surface to cause its ignition during a time interval of 20 μs is ~ 7.6 ± 0.6 mJ for the type-1 (batch B) composition. Similar experiments with the type-3 (batch A) composition gave a value of the minimum absorbed energy for ignition as 12.2 ± 1 mJ.

The results from the thermal ignition experiments are shown in figure 10, where the ignition time is plotted against the inverse of temperature of the MTV sample (type 2, batch A), 5 mm in diameter, 10 mm in thickness. The experimental points are well fitted by the equation

$$t_{ignition} = 9.072 \times 10^{-7} \exp\left(\frac{10954.95}{T}\right) \qquad \text{----------(1)}$$

where $t_{ignition}$ is the delay time and T the sample temperature; for a delay time to ignition of 20 μs,the required temperature is 3540 K. The ignition temperatures of MTV compositions (batch A) types 1, 2 & 3 were determined as 653, 593 and 683 K respectively.

According to the thermal theory of Zinn and Mader (1960), the time delay to ignition of an adiabatic energetic system at a temperature T is given by

$$t_{ignition} = \frac{C R T^2}{Q Z E} \exp(E/RT) \qquad \text{----------(2)}$$

where T is the initial sample temperature in K, C the heat capacity in $Jkg^{-1}K^{-1}$, Q the heat of reaction in $kJkg^{-1}$, Z thefrequency factor in s^{-1}, E the

activation energy in J mol^{-1}, and R the gas constant in J $mol^{-1}K^{-1}$. A comparison of equations (1) & (2) gives

$$E/R = 10954.95 \quad \text{---------- (3),}$$

and

$$CRT^2/QZE = 9.072 \times 10^{-7} \quad \text{---------- (4)}$$

From eq.(3), since R = 8.3 J $mol^{-1}K^{-1}$, we have E = 91.08 kJ mol^{-1}. The heat of reaction in our MTV samples is estimated, according to Kubota et al (1987), to be ~ 3168 $kJkg^{-1}$. Therefore, from eq.(4), and since T = 593 K, the frequency factor $Z = 5.5 \times 10^{10}\ s^{-1}$, which looks reasonable.

Finally, absorption spectra were taken of the MTV samples (type1, batch B) of different thicknesses in the wavelength range of 800 to 1200 nm; and in figure 11 the variation of the natural logarithm of the percentage transmission at the laser wavelength of 1060 nm vs the sample thickness is presented. The data points lie along a straight line from the slope of which the absorption coefficient is obtained as 3.8 cm^{-1}.

4. Discussion

The experiments described here have shown that an unfocused non-Q-switched laser pulse having a wavelength of 1060 nm can cause an ignition of small unconfined pellets of the MTV compositions. Also, the critical energy densities of the incident beam were determined to be in the range of 36 to 61 mJ mm^{-2} and the time delay to ignition between the beginning of the laser irradiation and the initiation of an ignition was measured to be ~ 20 μs.

In order to understand the mechanism of ignition, we first note that the optical absorption coefficient of 3.8 cm^{-1} of the MTV compositions is so small that at the critical energy density of the incident beam, the average temperature rise caused by the optical absorption of the laser radiation will not be high enough. For example at an incident energy density of 58 mJ mm^{-2} and ignoring reflection, the average temperature rise in a 100 μm thick surface layer will be only ~ 12 K. If, on the other hand, we assume that all the laser energy incident on an Mg particle is totally absorbed, we may make an approximate estimate of the adiabatic temperature rise of the particle. Since the thermal conductivity of Mg is very much higher than that of the PTFE matrix, it is justifiable to assume that

the temperature of the particle of radius of a few μm will be uniform. Under these conditions, the temperature rise ΔT of a particle of radius r is given by

$$\Delta T = \frac{3J}{4CrP} \qquad (5)$$

where J is the incident laser energy density, C the specific heat and ρ the density of Mg. Taking J = 6.1 mJ nm^{-2} (This is the energy density, which is emitted by the laser during the first 25 ms, which is the time delay to ignition, of the laser pulse. It has been estimated from the shape of the pulse and this energy is about 10% of the total output energy density), $\rho = 1.74 \times 10^3$ kg m^{-3}, C = 0.98 x 10^3 $Jkg^{-1}K^{-1}$ and r = 0.8 μm, we obtain,

ΔT = 3354 K.

This temperature rise is considerably higher than the ignition temperature of ~ 800 K of MTV compositions (see figure 10). In this calculation we have not taken account of the sub-microsecond structure of the laser pulse, as it will not affect the final adiabatic temperature rise of the Mg particle As said in the above, the exothermic reaction which is reponsible for causing ignition of the MTV compositions is between the Mg and the fluorine. Therefore, the ignition is most likely to be initiated at a Mg/polymer interface. Since the calculated temperature rise of the Mg particle exceeds the vaporization point (1363 K), it seems likely that there may also be exothermic reactions in the gaseous phase. However, from the photographic sequences we were not able to resolve whether the ignition initiated in the solid phase or the gaseous phase. Furthermore, it appears that during the life-time of a laser pulse the absorption coefficient may increase due to the polymer thermal degradation/decomposition, but at this stage it is difficult to estimate this change. Our values of the minimum absorbed energies which give rise to ignition are therefore quite likely to be underestimates.

Using purely thermal ignition experiments, we have shown (see figure 10) that the time delay, $t_{ignition}$, to ignition of the MTV compositions follows equation (1). For a measured time delay of 20 μs from our laser ignition experiments, the required sample temperature is 3540 K. This value of the 'hot-spot' temperature is quite close to the value of 3648 K of the estimated temperature of a 8 μm radius Mg particle. This correlation between the measured time to ignition and the estimated temperature rise of an Mg particle suggests that the mechanism of laser ignition is thermal. That is, the incident laser light is

heavily absorbed at the Mg particle in the composition, resulting in the rise of temperature and consequent initiation of ignition.

We also found that at relatively low incident laser beam energies, ignition only occurred at the second, third, or the fourth irradiation at the same area of the sample (see table 1). This observation is explained on the fact that at a sub-threshold incident energy density, some darkening of the MTV sample around the Mg particles occurs (see figure 7); the degree of this darkening increases at subsequent irradiations. An effect of the darkening is that this will cause an increase in the surface absorption coefficient which will give rise to higher surface temperatures of the polymers surrounding an Mg particle due to the laser irradiation and consequently a higher probability of ignition, as observed in these experiments.

5. Conclusions

It has been shown that an unfocused non Q-switched laser pulse of wavelength λ =1060 nm can ignite our MTV compositions. The ignition occurs at isolated microscopic regions, which are probably magnesium particles. It has been suggested that ignition by laser irradiation is thermal in origin.

References

De Yong L V and Valenta F J 1989 Proc. 14th Int. Seminar. Pyrotechnics (Jersey, Channel Islands) (Royal Armament Research and Development Establishment, Fort Halstead, U.K.) pp 123–33

Dierks B V 1986 J. Hazardous Materials 13 3–15

Habersat J 1981 JANNAF Safety and Environmental Protection Sub-committe Meeting, (Orlando:Kennedy Space Centre, Florida) pp 13.

Hagan J T and Chaudhri M M 1981 J. Mater. Sci. 16 2457–466

Haq I U and Chaudhri M M 1989 Proc. 14th Int. Seminar. Pyrotechnics (Jersey, Channel Islands) (Royal Armament Research and Development Establishment, Fort Halstead, U.K.) pp 135–43

Holy J A and Girmann T C 1988 Proc. 13th Int. Seminar Pyrotechnics (Colorado) (Chicago: ITT Research Institute) pp 449–67

Kubota N and Serizawa C 1987 Propellants, Explosives, Pyrotechnics. 12 145–8

Oestmark H 1985 Proc. 8th Symp. (Int.) on Detonation (Albuquerque) (Naval Surface Weapons Centre, White Oak, Silver Spring, MD) pp 473–81

Potter L J 1988 Proc. 13th. Int. Seminar. Pyrotechnics (Colorado) (Chicago: ITT Research Institute) pp 639–59

Shin F G Tsui W L and Yeung Y Y 1989 J. Mater.Sci. 8 1383–5

Zinn J and Mader C L 1960 J. Appl. Phys. 31 323–8

Acknowledgements

The authors would like to thank Dr. J. N. Towning and Mr. B. Hammant of RARDE, Fort Halstead, for helpful discussions. This work has been carried out with the support of the Ministry of Defence, Procurement Executive. One of us (IUH) would like to thank the M.O.D and the SERC for a CASE award.

Table 1. Minimum incident critical energy densities for ignition of MTV (batch A) samples. All the samples have the same dimensions; diameter: 5mm;thickness: 4mm. The error in the energy density results is ± 8%. (note that these energy values were determined when there was no filter in the path of the laser beam).

MTV -type	Incident energy density /mJ mm^{-2}	laser shot No.	No.of experiments	absorbed ignition energy density /mJ mm^{-2}	ignition energy (actually absorbed) /mJ
1	58.5	1st	3	1.73	12.2
"	52.2	2nd	20	*	*
2	60	1st	2	1.78	12.5
"	52.2	3rd	20	*	*
3	61.2	1st	1	1.81	12.8
"	52.2	4th	15	*	*

*— these values could not be estimated as we do not know the reflectivity of the darkened surfaces.

Table 2. Minimum incident critical energy densities for ignition of (batch B) MTV samples. All the samples were 5 mm in diameter; the ignition behaviour was independent of the pellet thickness.The error in the energy density results is ± 8%. (note that to measure the energies shown below, the laser beam passed through a filter transmitting above 780 nm before falling on the test sample).

MTV-type	Incident energy density /mJ mm^{-2}	laser shot No.	No.of experiments	event	absorbed ignition energy density /mJ mm^{-2}	ignition energy (actually absorbed) /mJ
1	36.5	1st	15	ignition	1.08	7.6
2	36.5	1st	15	ignition	1.08	7.6
3	36.5	up to 20th	10	no ignition	–	–

Figure Captions

Figure 1. Oscilloscope trace of the laser and sync. pulses. The laser intensity is shown by the arbitrary scale on the left, whereas the scale on the right refers to the sync. pulse.

Figure 2. Schematic diagram of the laser and camera arrangement.

Figure 3. Schematic diagram of the photodiode set up for recording the light emission from an ignition.

Figure 4. Oscilloscope trace of the light output due to ignition of an MTV pellet (type 1, batch B). Sample diameter: 5 mm; thickness: 2mm. The sync. pulse from the control unit is also shown. Incident beam energy: 0.52 J. The scale on the left refers to the signal from the photodiode in arbitrary units, whereas the scale on the right refers to the sync. pulse.

Figure 5. Schematic diagram of the set up for measuring the delay time to ignition.

Figure 6. Schematic diagram of the hot-plate arrangement for studying the thermal ignition of the MTV compositions.

Figure 7. SEM micrograph showing the laser beam damage on the surface of an MTV pellet (type 1, batch A). The arrows refer to: (a), burnt polymer; (b), site of ejected Mg particle; (c), undamaged Mg particles.

Figure 8. Selected frames from a sequence of high-speed photographs of the initiation and propagation of ignition in a pellet of MTV (type 1, batch A) by a non Q-switched unfocused laser pulse. The laser beam impacted the sample in frame 1, causing ignition. The ignition front is shown at arrows in frames 3, 15, 117, 119 & 225. Interframe time: 0.15 ms; sample diameter: 5 mm; sample thickness: 3 mm; The lateral width of each frame is 4.4 mm. The number of every frame is given on its left side.

Figure 9. A selected Imacon Camera sequence of the initiation and propagation of an ignition in a pellet of MTV (type 3, batch A) by a non Q-switched unfocused laser pulse irradiating the same sample area for the 4th time in frame 1. The dark region in this frame is formed by the previous three laser shots. The emission of light which occurs in frame 2, represents the initiation of an ignition. Interframe time: 20 μs. The number of every frame is given on its left bottom side. The time interval between two consecutive laser shots was 5 – 7 minutes.

Figure 10. Ignition time versus inverse temperature of MTV (type 2, batch A) samples. Thickness: 10 mm; diameter: 5 mm.

Figure 11. The variation of the percentage transmission of light of wavelength 1060 nm with the thickness of MTV samples.

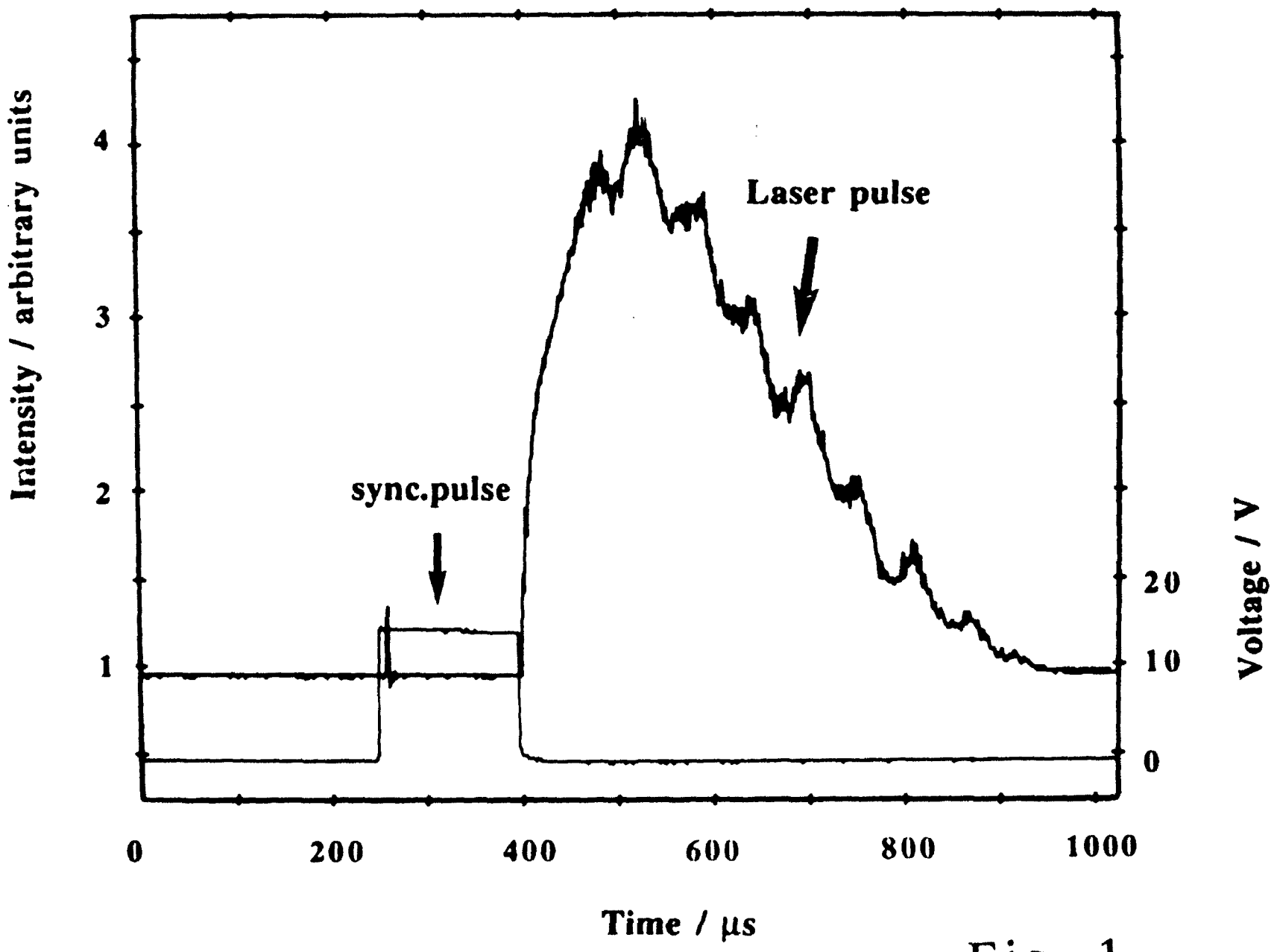
Intensity / arbitrary units
4
3
2
1
Laser pulse
sync.pulse
20
10
0
Voltage / V
0
200
400
600
800
1000
Time / µs

Fig. 1

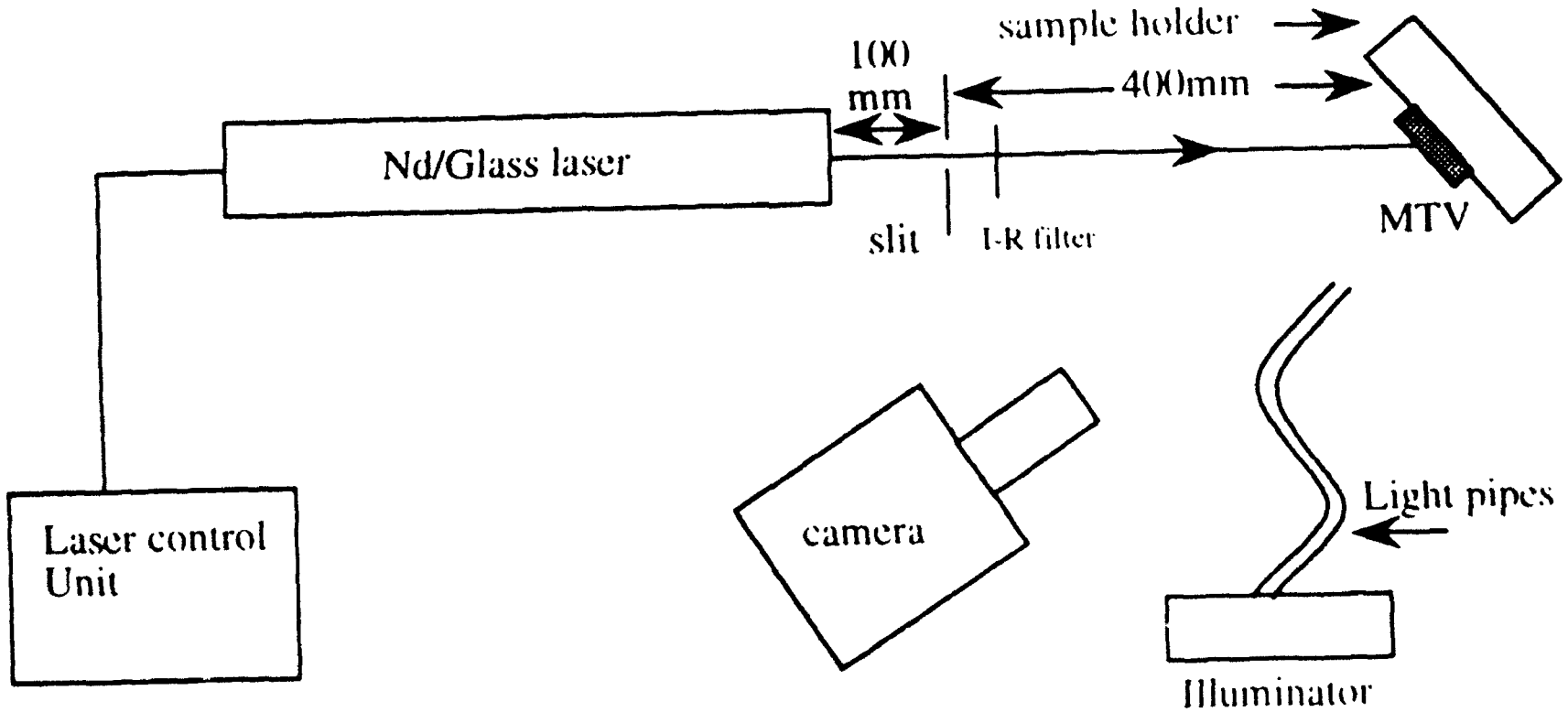
sample holder
100
mm
400mm
Nd/Glass laser
slit
I-R filter
MTV
Laser control
Unit
camera
Light pipes
Illuminator

Fig. 2

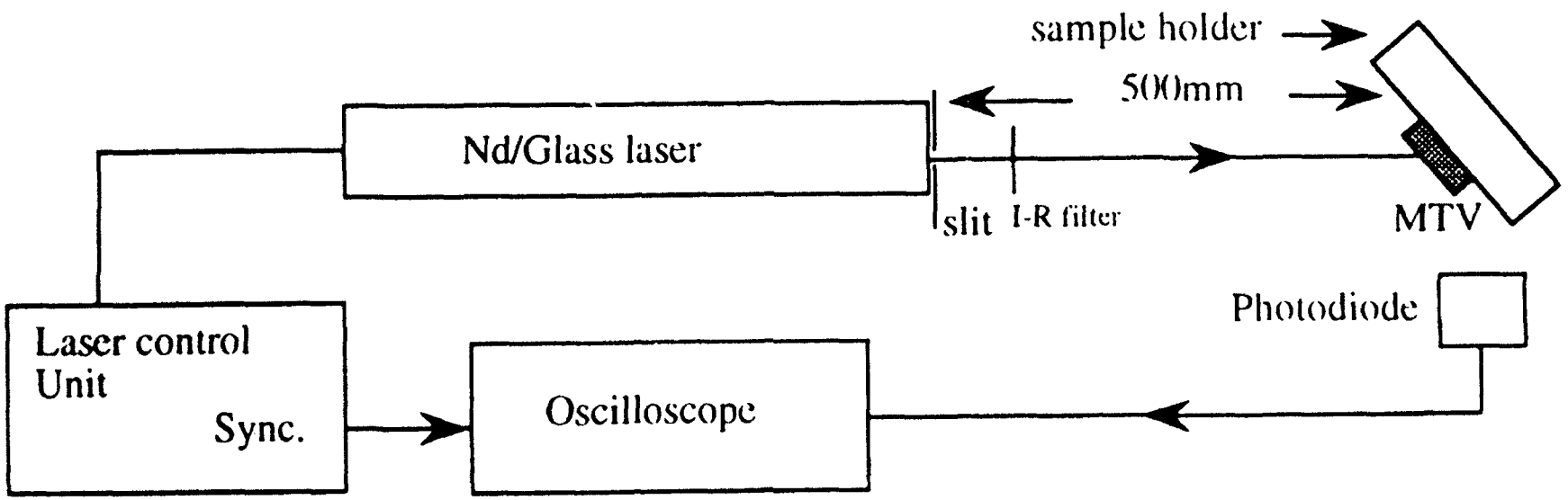
sample holder
500mm
Nd/Glass laser
slit
I-R filter
MTV
Photodiode
Laser control
Unit
Sync.
Oscilloscope

Fig. 3

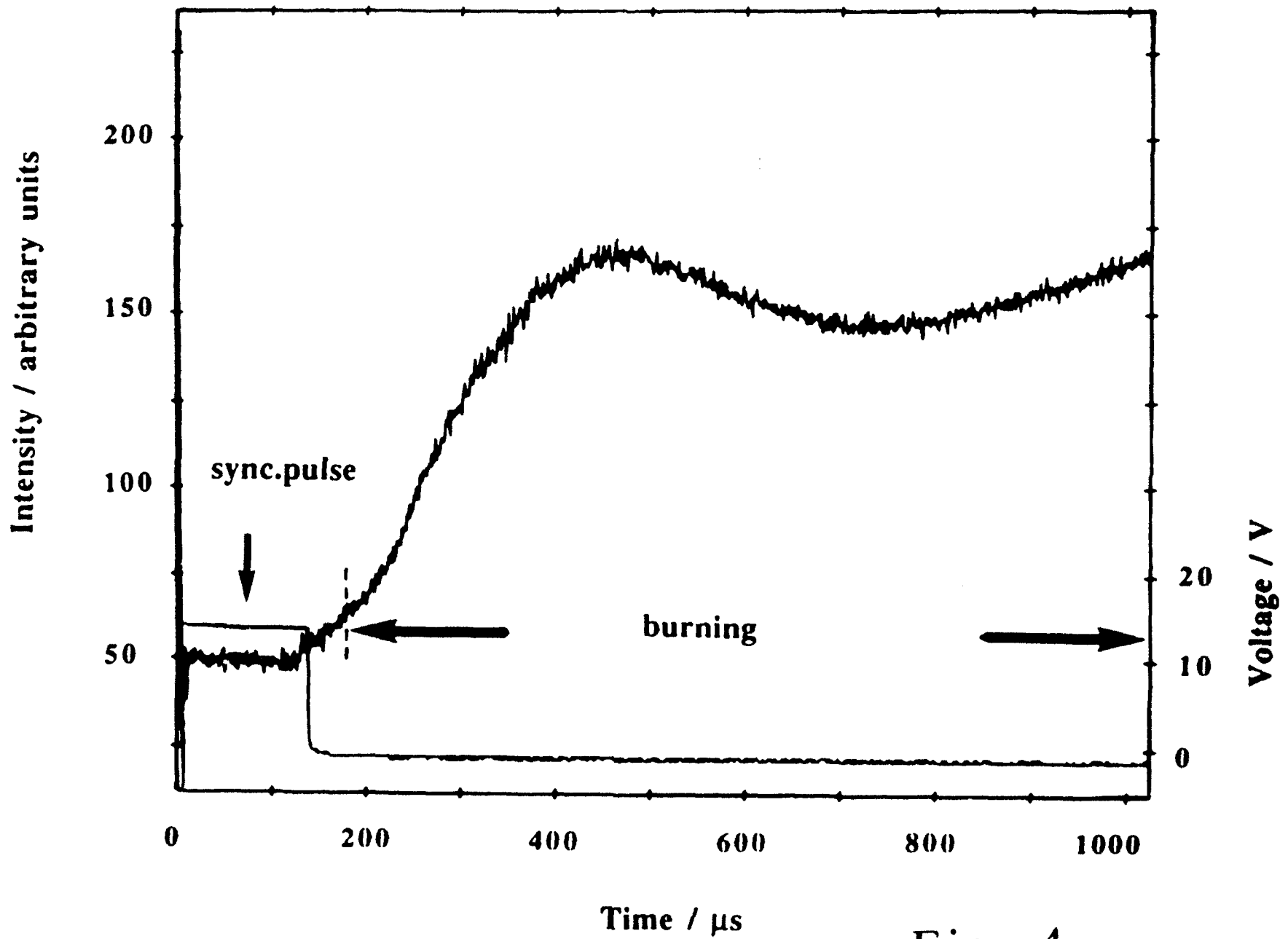
Intensity / arbitrary units
200
150
100
50
sync.pulse
burning
20
10
0
Voltage / V
0
200
400
600
800
1000
Time / µs

Fig. 4

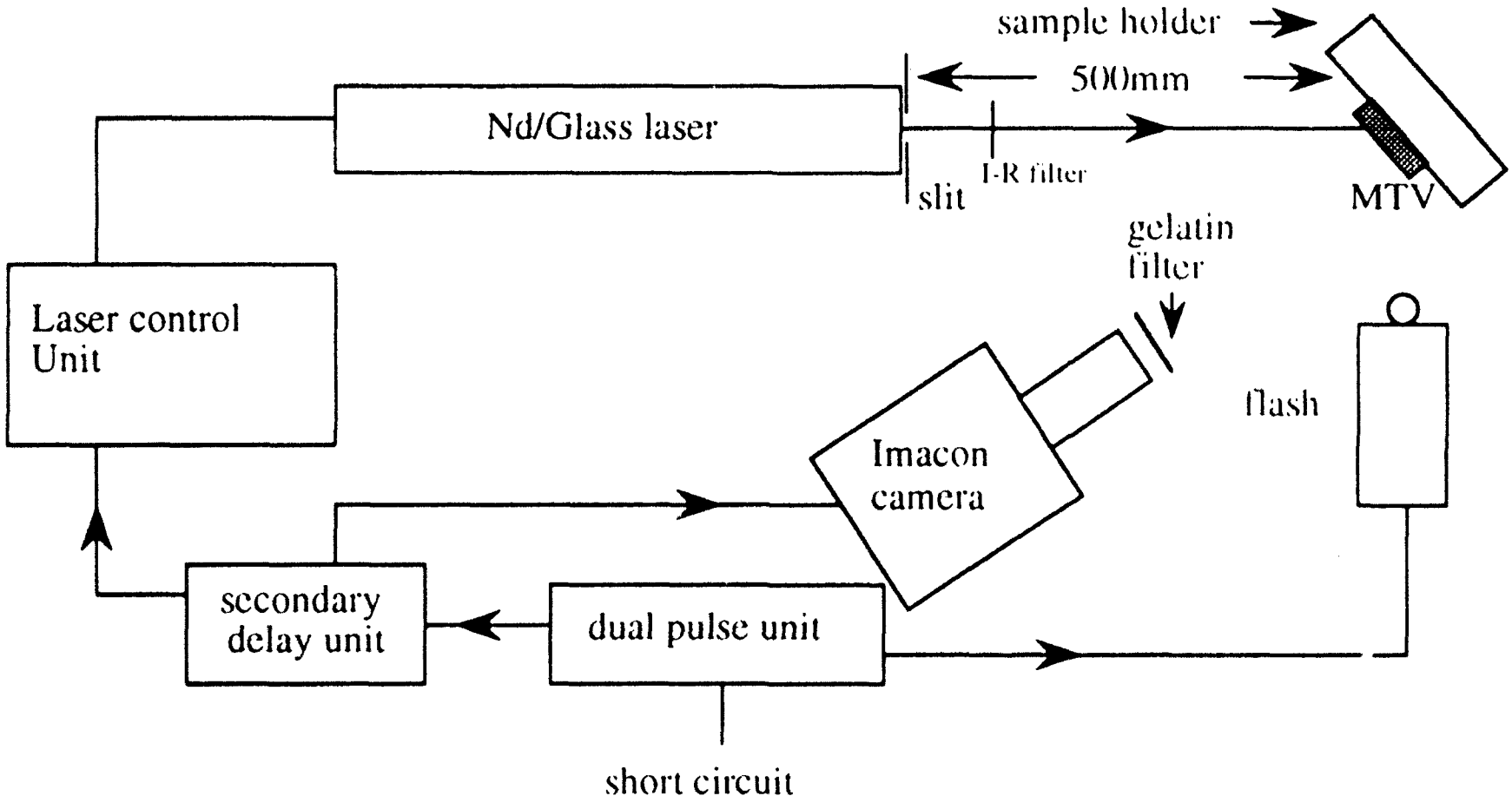
sample holder
500mm
Nd/Glass laser
slit
I-R filter
MTV
gelatin
filter
Laser control
Unit
flash
Imacon
camera
secondary
delay unit
dual pulse unit
short circuit

Fig. 5

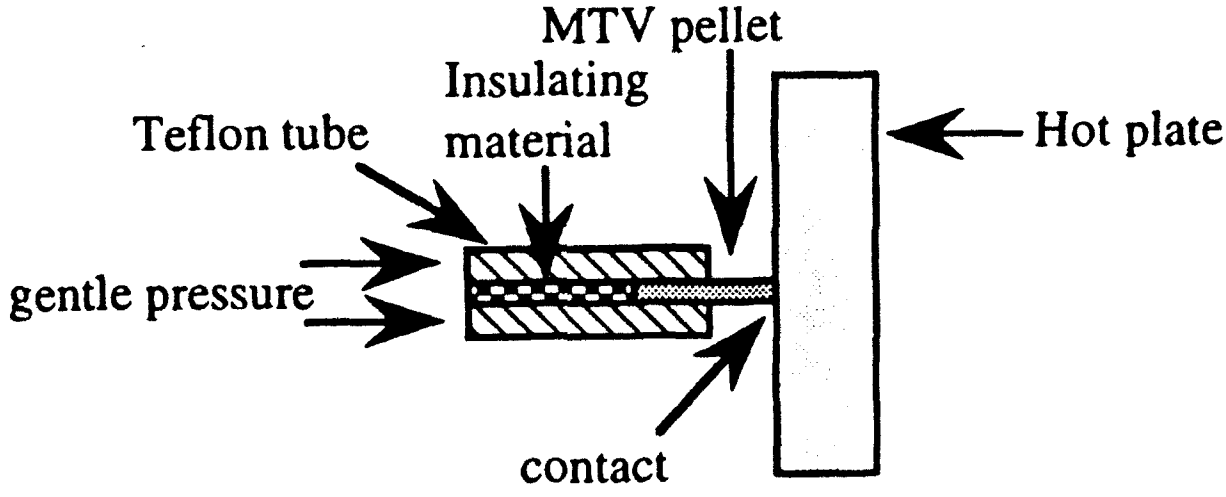
MTV pellet
Insulating material
Teflon tube
Hot plate
gentle pressure
contact

Fig. 6

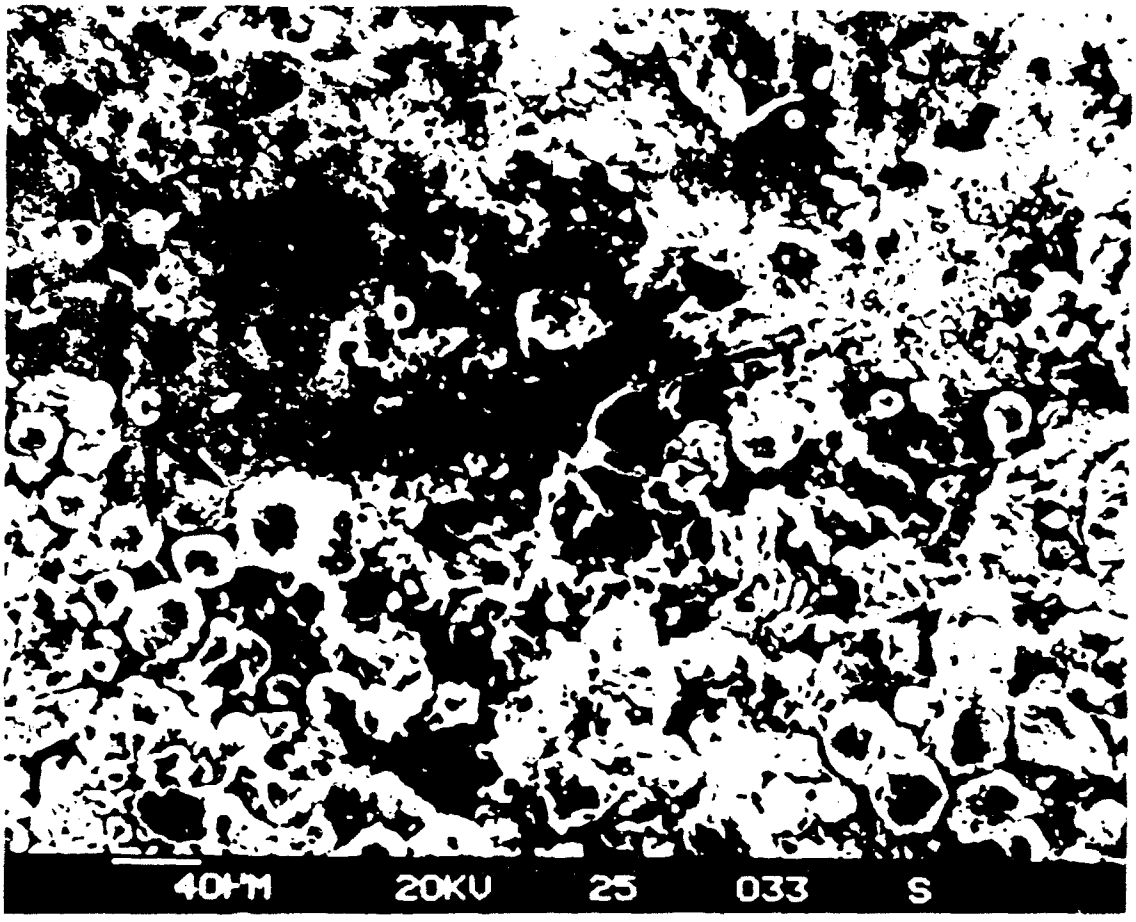

Fig. 7

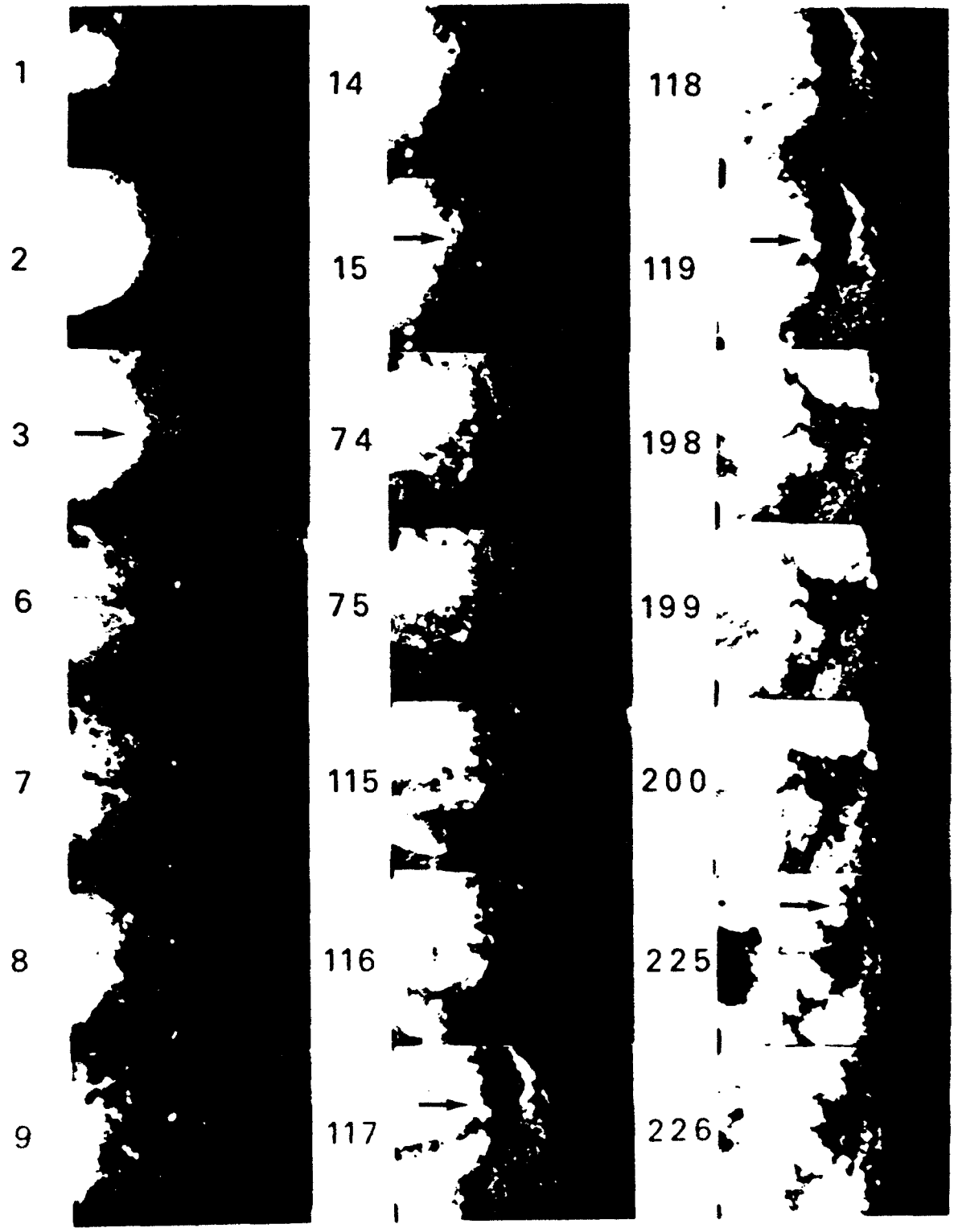

Fig. 8

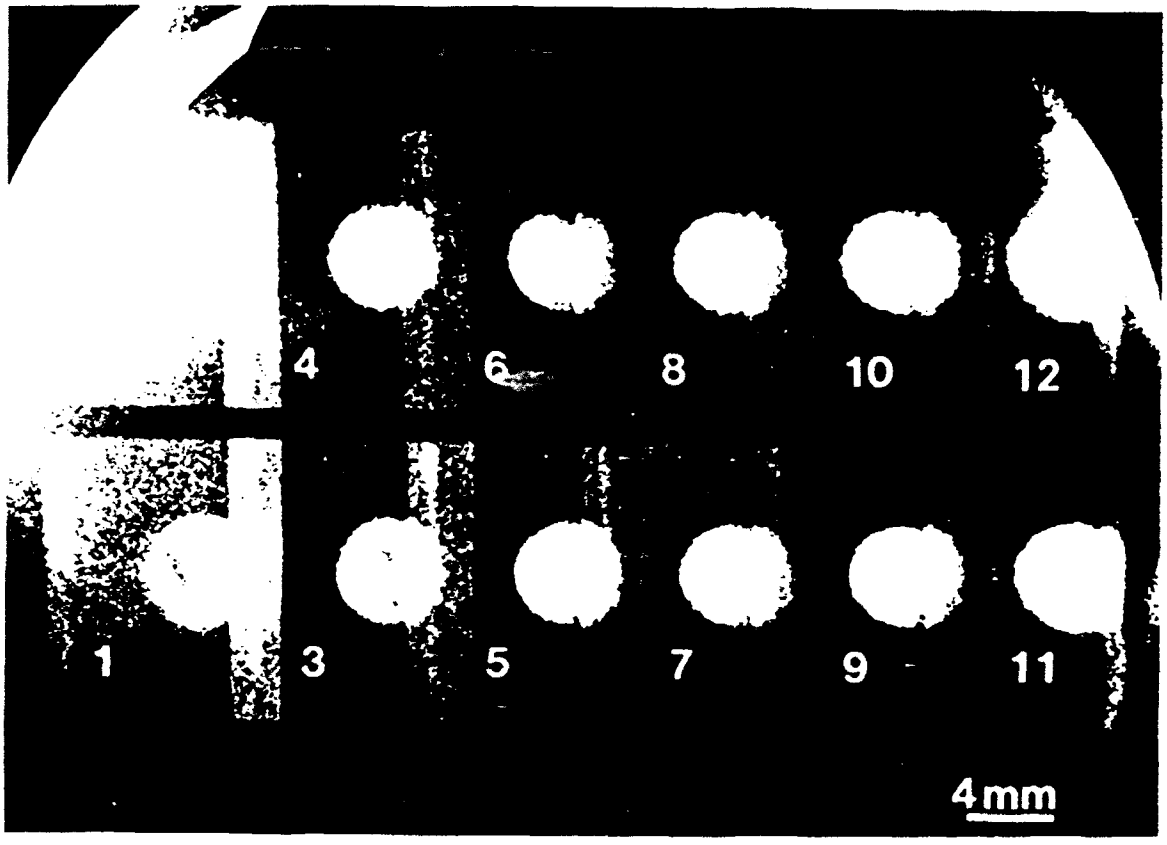

Fig. 9

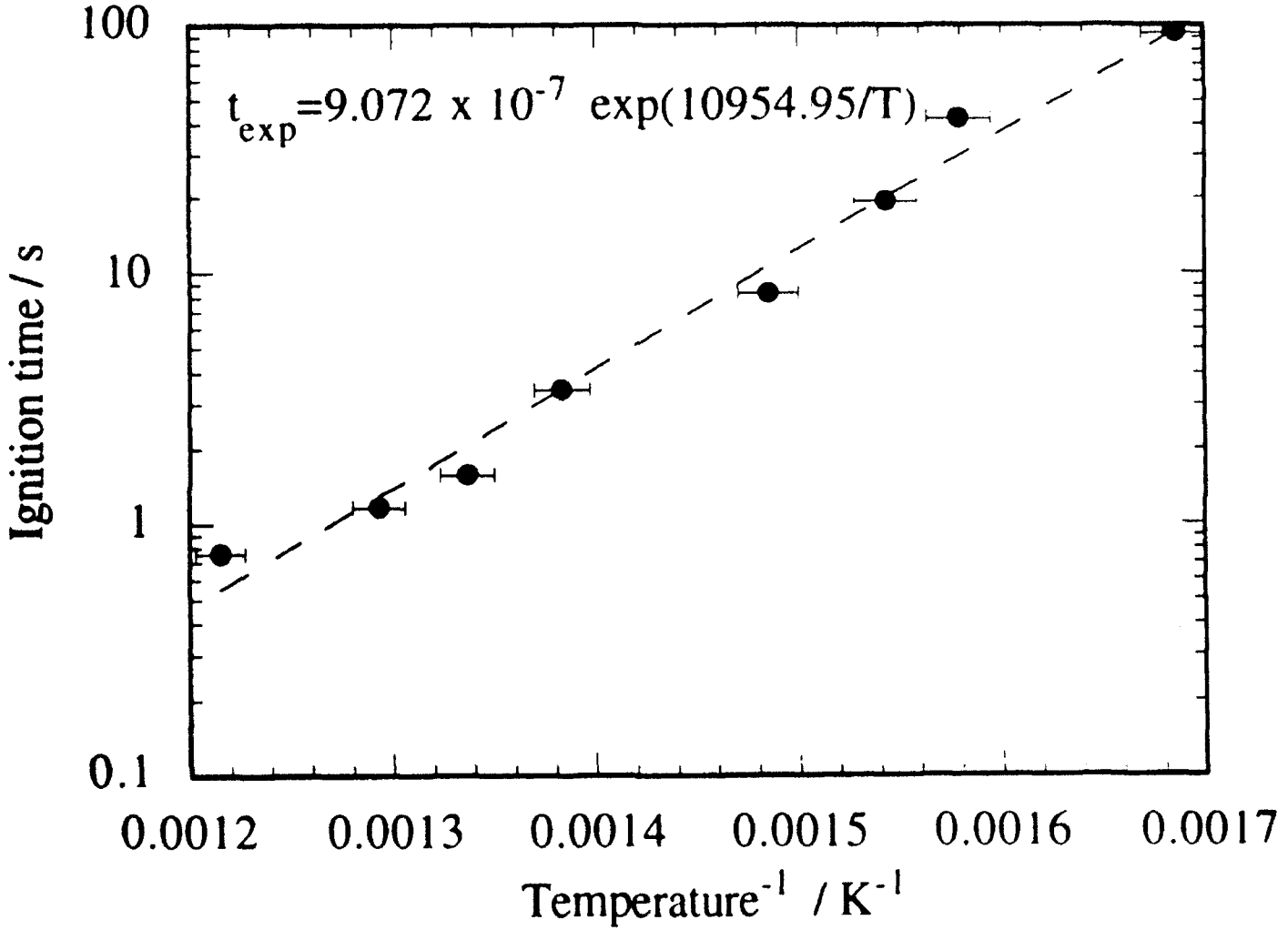
100
10
1
0.1
t_{exp}=9.072 x 10^{-7} exp(10954.95/T)
Ignition time / s
0.0012
0.0013
0.0014
0.0015
0.0016
0.0017
Temperature^{-1} / K^{-1}

Fig. 10

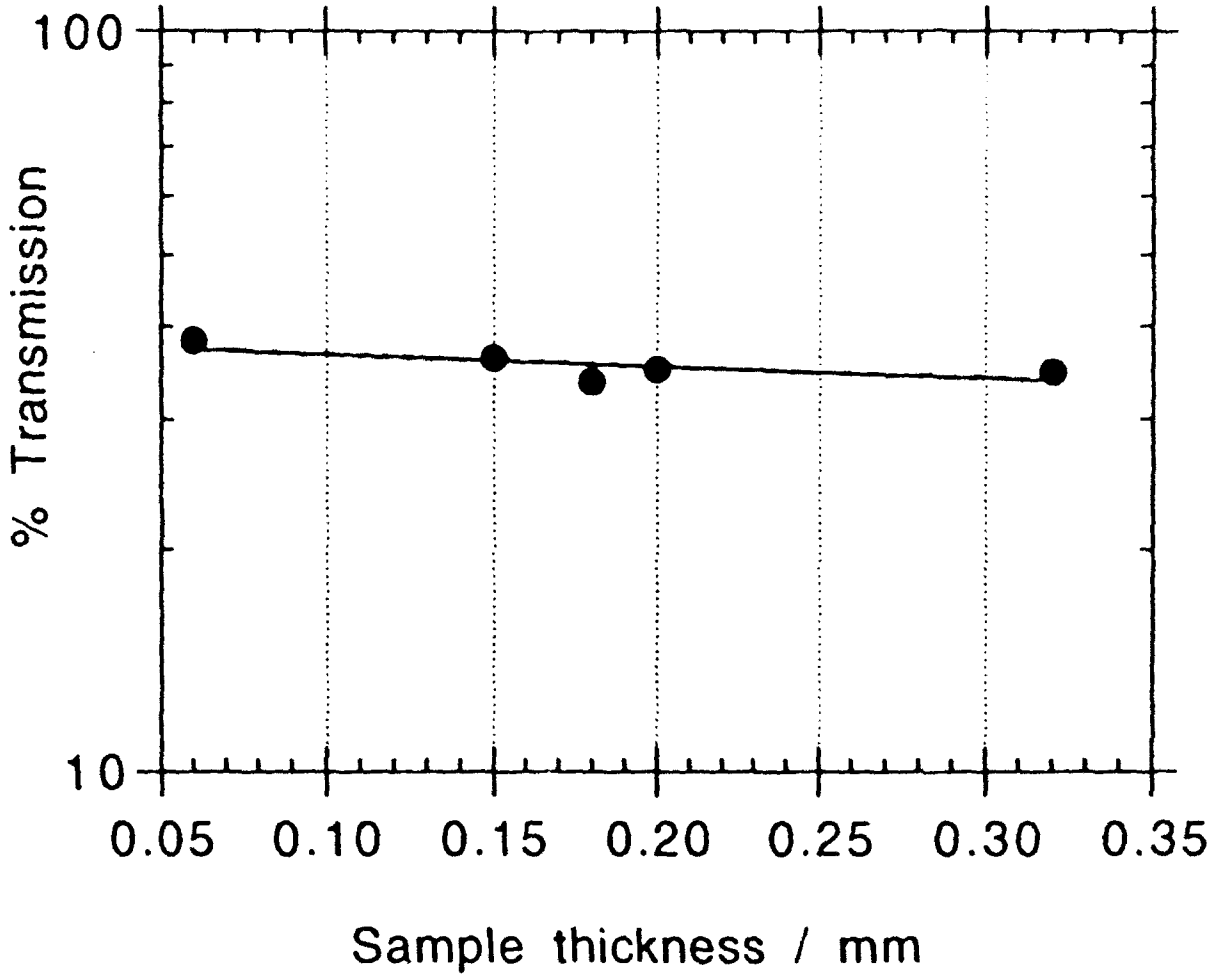
100
10
% Transmission
0.05
0.10
0.15
0.20
0.25
0.30
0.35
Sample thickness / mm

Fig. 11